REPORT DOCUMENTATION PAGE

Form Approved
OMB No. 0704-0188

1. AGENCY USE ONLY (Leave blank)	2. REPORT DATE	3. REPORT TYPE AND DATES COVERED
	27 Dec 95	

4. TITLE AND SUBTITLE

Spectral Characteristics of an Aerogel

5. FUNDING NUMBERS

6. AUTHOR(S)

Robert Joseph Morrison

7. PERFORMING ORGANIZATION NAME(S) AND ADDRESS(ES)

AFIT Students Attending:

Arizona University

8. PERFORMING ORGANIZATION REPORT NUMBER

95-144

9. SPONSORING/MONITORING AGENCY NAME(S) AND ADDRESS(ES)

DEPARTMENT OF THE AIR FORCE
AFIT/CI
2950 P STREET, BLDG 125
WRIGHT-PATTERSON AFB OH 45433-7765

10. SPONSORING/MONITORING AGENCY REPORT NUMBER

11. SUPPLEMENTARY NOTES

12a. DISTRIBUTION/AVAILABILITY STATEMENT

Approved for Public Release IAW AFR 190-1
Distribution Unlimited
BRIAN D. Gauthier, MSgt, USAF
Chief Administration

12b. DISTRIBUTION CODE

13. ABSTRACT *(Maximum 200 words)*

14. SUBJECT TERMS	15. NUMBER OF PAGES 67
	16. PRICE CODE

17. SECURITY CLASSIFICATION OF REPORT	18. SECURITY CLASSIFICATION OF THIS PAGE	19. SECURITY CLASSIFICATION OF ABSTRACT	20. LIMITATION OF ABSTRACT

SPECTRAL CHARACTERISTICS OF AN AEROGEL

by

2LT Robert Joseph Morrison, USAF

For the Degree of Master of Science in Physics

1995

67 Pages

The University of Arizona

ABSTRACT

The spectra of an aerogel bombarded with high energy (0.5-1.0 MeV) protons, H_2^+, and H_3^+ have been measured and investigated. The spectra from the excited gel are essentially continua peaking in the blue (λ4500 Å), and cannot be explained by the spectral lines from known participating elements or a blackbody. They are due to luminescence. Wavelength scans taken before, inside, and behind the gel gave different spectra. The continuum's spatial intensity was independent of the particle energy, but the location of the intensity maximum moved further downstream inside the gel as the particle energy increased. The spatial intensity maintained the same shape, but its shape depended on the wavelength viewed. Instantly after the beam initially strikes the gel, a large explosion of light is emitted. The burst is followed by a very fast (0.8 sec) and then slower (4 sec) decay of radiation λ4500 Å, which depended on wavelength.

WORKS CITED

"Aerogels: Solid Pieces of Nothing." Compressed Air Magazine. June 1989: 27-31.

Anderson, Kevin J. "Historical Note: From Aqua Gel to Aerogel." MRS Bulletin. March 1991: 63-64.

Bashkin, Stanley, ed. Beam-Foil Spectroscopy. 2 Vols. New York: Gordan, 1968. Vol. 2.

Bashkin, Stanley, ed. Beam-Foil Spectroscopy: Proceedings of the Third International Conference on Beam-Foil Spectroscopy. Amsterdam: North-Holland, 1973.

Becker, Ralph S. Theory and Interpretation of Fluorescence and Phosphorescence. New York: Wiley Interscience, 1969.

Birks, J. B. The Theory and Practice of Scintillation Counting. New York: Macmillan, 1964.

Curran, S. C. Luminescence and the Scintillation Counter. New York: Academic, 1953.

Delaney, G. F. G., and E. C. Finch. Radiation Detectors: Physical Principles and Applications. Oxford: Clarendon, 1992.

Humphries, Stanley, Jr. Principles of Charged Particle Acceleration. New York: Wiley & Sons, 1986.

Hunt, Arlon. "Aerogels: The Lightest Solid." Encyclopedia Britannica 1995 Science Year Book.

Instruction Manual HVI-475M1: The Model AN-2000 Positive Ion Accelerator. HV Engineering: Burlington, n.d.

Kahn, Jeffery. "Innovative Insulators." LBL Research Review. Summer 1991: 2-9.

Scanning Monochrometer EU-700 and EUE-700 Series. Benton Harbor: Heath, 1969.

Serway, Raymond A., Clement J. Moses, and Curt A. Moyer. Modern Physics. Philadelphia: Saunders College, 1989.

Svanberg, Sune. Atomic and Molecular Spectroscopy: Basic Aspects and Practical Applications. Vol. 6 of Springer Series on Atoms+Plasmas. 8 Vols. Heidelberg: Springer-Verlae, 1991.

Tatarskii, V. I., et al, ed. Wave Propagation in Random Media (Scintillation). Bellingham: SPIE, 1993.

Weber, Marvin J., et al, ed. Scintillator and Phosphor Materials. Vol. 348 of Materials Research Society Symposium Proceedings. Pittsburg: MRS, 1994.

Williams, W. S. C. Nuclear And Particle Physics. Oxford: Clarendon, 1991.

SPECTRAL CHARACTERISTICS OF AN AEROGEL

by

2LT Robert Joseph Morrison, USAF

A Thesis Submitted to the Faculty of the

DEPARTMENT OF PHYSICS

In Partial Fulfillment of the Requirements
For the Degree of

MASTER OF SCIENCE

In the Graduate College

THE UNIVERSITY OF ARIZONA

1 9 9 5

STATEMENTS BY THE AUTHOR

This thesis has been submitted in partial fulfillment of the requirements for an advanced degree at the University of Arizona and is deposited in the University Library to be made available to borrowers under the rules of the Library.

Brief quotations from this thesis are allowed without special permission, provided that accurate acknowledgment of source is made. Requests for permission for extended quotation from or reproduction of this manuscript in whole or in part may be granted by the head of the major department or the Dean of the Graduate College when in his or her judgment the proposed use of the material is in the interest of scholarship. In all other instances, however, permission must be obtained from the author.

SIGNED: _____

APPROVAL BY THESIS DIRECTOR

This thesis has been approved on the date shown below:

_____ _____

William S. Bickel Date
Professor of Physics

ACKNOWLEDGMENTS

I wish to express my sincerest appreciation to Professor William S. Bickel for being my Thesis Advisor. Without his guidance, wisdom, and understanding this Thesis would have never been possible.

To my immediate family, without their undying support in all my endeavors I would have been lost a long time ago. Especially my mother and father, they were always there to support and comfort me, as parents and true friends.

To my friends, both new and old, sharing war stories and personal heartaches always made the time seem a little more bearable. To Joe Kendall goes a special thanks, him and the Cactus Moon helped keep my sanity. And Susan Day for being a very near and dear friend that will be greatly missed as I move on to my next adventure in life.

To the United States Air Force, for making this whole thing possible. The numerous military personnel at Davis-Monthan AFB, the ROTC Detachment, and the Air Force Institute of Technology that were always there to lend a helping hand. May this be the start of a long and fruitful career.

TABLE OF CONTENTS

LIST OF FIGURES

ABSTRACT

The spectra of an aerogel bombarded with high energy (0.5-1.0 MeV) protons, H_2^+, and H_3^+ have been measured and investigated. The spectra from the excited gel are essentially continua peaking in the blue (λ4500 Å), and cannot be explained by the spectral lines from known participating elements or a blackbody. They are due to luminescence. Wavelength scans taken before, inside, and behind the gel gave different spectra. The continuum's spatial intensity was independent of the particle energy, but the location of the intensity maximum moved further downstream inside the gel as the particle energy increased. The spatial intensity maintained the same shape, but its shape depended on the wavelength viewed. Instantly after the beam initially strikes the gel, a large explosion of light is emitted. The burst is followed by a very fast (0.8 sec) and then slower (4 sec) decay of radiation λ4500 Å, which depended on wavelength.

1. STATEMENT OF OBJECTIVE

Spectroscopy has developed over the years in order to extract as much information as possible from electromagnetic waves. The spectral emissions from a star properly analyzed can give information about topics ranging from the star's composition to it's rotational and orbital velocities. Spectral emissions from a gas can be used to discover its identity, and if it contains more than one element, the relative composition and interaction between its components can sometimes be determined. Figure 1 shows the spectrum from a preliminary wavelength scan of an aerogel. The goal is to unlock the secrets that the gel spectrum holds and find out everything possible about the aerogel.

With all of the information that has been obtained by analyzing spectral emissions, this powerful experimental tool is being used to shed light on an unknown, an aerogel. The first question to be answered: "What is an aerogel?" Since our goal is to see how an aerogel interacts with a particle beam, we will compare its properties with those of other substances that have been used for particle beam interaction. We will also examine possible sources of radiation that can be created by the beam-gel interaction. Then we will discuss the experimental set-up and methods. We will compare the various radiation sources with the spectra from the beam-gel excitation. We conclude by suggesting some areas for further research.

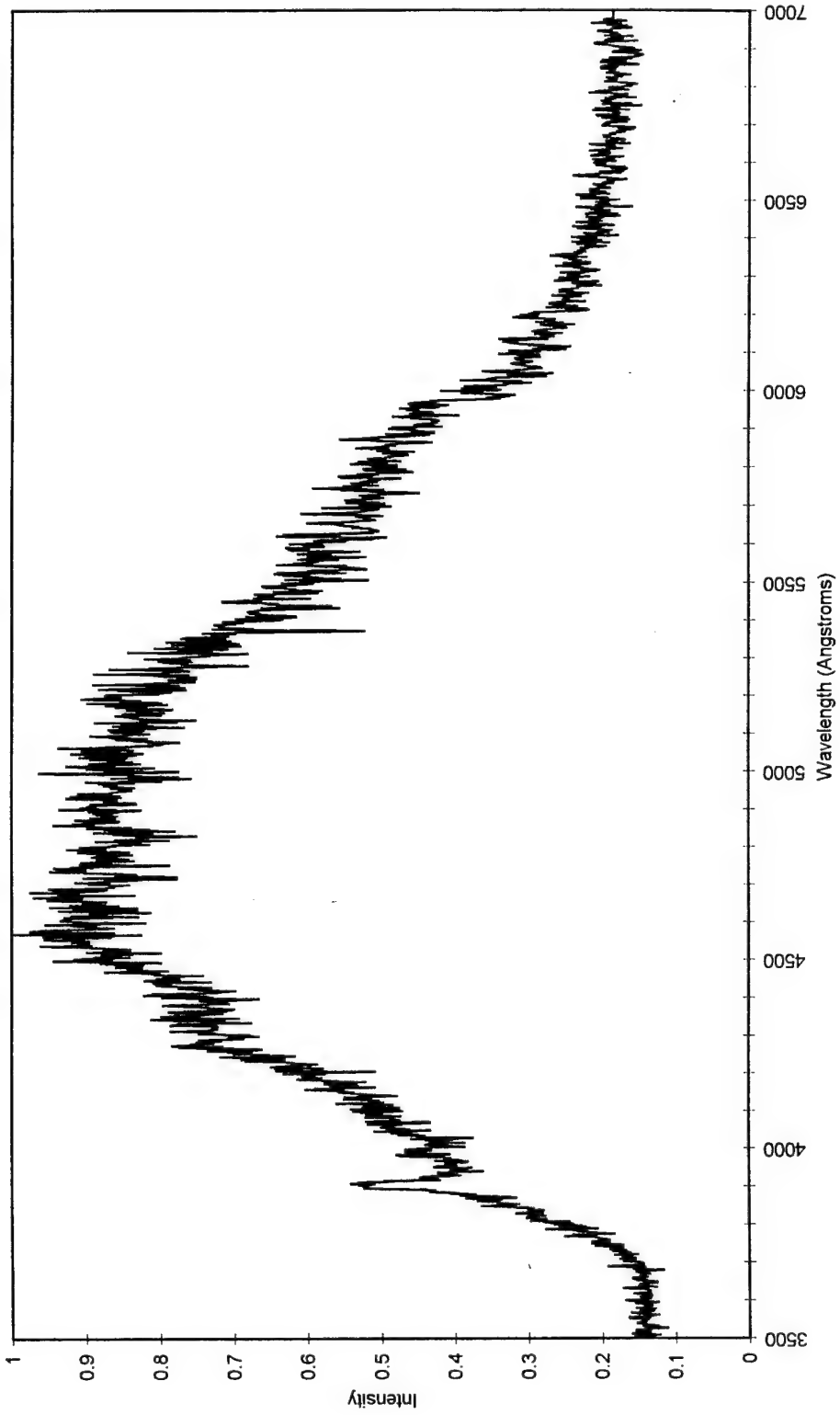

Figure 1: Initial spectrum of a 5E-7 A, 0.5 MeV H3+ excited gel (P=1.2E-4 torr) observed 1 mm inside the gel.

2. BACKGROUND INFORMATION ON AEROGELS

Aerogels are unique solids that are equivalent to suspended molecules of gas. They are transparent, with a composition of mostly air, yet they have an intricate structural lattice that gives them form. They have unique properties and characteristics that make them difficult to categorize with other substances like gases, liquids, and solids. Since gels cannot be neatly categorized, particle interaction with gels should make an intriguing spectroscopic study.

2.1. Aerogel Production

Aerogels were first created by S. S. Kistler in the 1930's.[1] He started the process by mixing a solution of sodium silicate, Na_4Si0_4, with hydrochloric acid, HCl. The solution was left to coagulate for a day so the actual gel structures could form. Next the hydrochloric acid was washed out of the gel using water, coining the term aqua gel. The new solution was then placed in alcohol because water would dissolve the gel at the higher temperatures used later in the process. The gel was referred to as an alco gel during this phase.

Gels are naturally-occurring phenomena. They are found in a lot of food products including, for example, eggs, puddings, and Jell-O. The difficulty lies in extracting the gel from the liquid that it is submerged in. As the liquid

starts to evaporate from the gel, surface tension builds, creating concave menisci that cause the gel structure to collapse as the liquid is drawn out of the gel. The final solution was to turn the liquid into a supercritical fluid which has no surface tension. This is done by subjecting the alco gel to a high temperature and pressure in an autoclave and allowing it to dry without the destructive effects of the surface tension. For methanol, the alcohol used, the alco gel is subjected to a pressure of 6.1×10^4 torr, or 8.1×10^6 N/m^2, and a temperature of $513^{\circ}K$ in the autoclave.

This very slow and time consuming process could produce only small quantities at a time. In the 1960's, the aerogel was seen as a means to store rocket fuel, but a better method for producing gels had to be found. Stanislas J. Teichner did just that and coined the new word, sol gel. He used tetramethoxysilane (TMOS), $Si(OCH_3)_4$, an alkoxide, a silicon atom surrounded by four alcohol atoms.[2] The TMOS was mixed with water and then an acid or base catalyst was added. The product was silicic acid and methanol which was left to coagulate. Time for the process to occur depended on the catalyst used. The pH and concentration of the solution could be varied to control the final density and structure of the sol gel.

This proved to be a much faster process, capable of producing large quantities of gel at a time, but the methanol at the temperatures and pressures being used was volatile. Arlon J. Hunt replaced the TMOS with tetraethoxysilane (TEOS), $Si(OC_2H_5)_4$.[3] Instead of having silicic acid and methanol, the solution was now silicic acid and liquid carbon dioxide. This got rid of the volatile methanol and also brought the temperature for drying down to 303°K. The process can take from 20 minutes to 2 months, depending on the catalyst used.[4]

2.2. Aerogel Dimensions and Characteristics

Aerogels are solid, transparent "nothing". They are most commonly made of silica, SiO_2, but they have been made from metal oxides (iron and tin), alumina, zirconia, titania, magnesia, gelatin, organic polymers, natural gels, and carbon.[5] Figure 2 is a micrograph of the aerogel showing its high porosity and its cross linked structure. The interconnected microstructure of the gel has dimensions smaller than 100 Å, which is much smaller than the wavelength of visible light. It was found that the structure's pattern is a fractal, self-similar at different scale lengths.[6] Gels have an ultra-fine pore size smaller than 1000 Å. The porosity i.e. the percent of open space to actual structure of the gels was 98% in the 1930's. Today gels can be made 99.9% porous. The large porosity, gives

Figure 2: Micrograph Of Aerogel[7]

1000 m^2 for the total surface area for one gram of aerogel.[8] The density of the material ranges from $3x10^{-2}$ to $3x10^{-1}$ g/cm^3, ($\rho_{air} = 1.2x10^{-3}$ g/cm^3), with refractive indices varying from 1.3 to as low as 1.002 ($n_{air} = 1.000293$).[9]

This "nothing" substance has several characteristics that are not intuitively obvious. Its thermal conductivity is two orders of magnitude lower than the 0.8 for silica glass. This low value can be improved by 90% evacuation of air which also makes the aerogel stronger. The speed of sound in the gel ranges from 100 to 300 m/sec ($v_{air} \approx 330$ m/sec), which is typical of materials such as rubber. For comparison, the speed of sound in silica glass is 5000

m/sec. The speed of sound decreases as a mechanical stress is applied to the gel, which is opposite of what is observed with normal solids. The gel can be transparent, but usually it has a slight color tint. The usual blue coloring is caused by Rayleigh scattering (which also accounts for why the sky is blue) from the inconsistencies in the pore sizes.[10] By controlling the manufacturing process and limiting the number of large pores, the gel can be made clearer and more transparent. The various procedures and parameters used in the manufacturing process can be manipulated to create aerogels with the desired properties.

2.3. Aerogel Uses

Aerogels make very efficient thermal insulators. With the new chlorinated fluorocarbon (CFCs) laws, aerogels are being used in refrigerators by using micro-pellets that retain most of the gels' characteristics.[6] More transparent gels with higher structural integrity are being designed for possible window insulation. Aerogels are used to collect micro meteoroids in their ultra-fine structure. Different versions of the gel can be used in fire retardents. Gels are used in high energy particle detectors, such as for Cherenkov radiation in the 0.8 to 30 GeV range. Their peculiar acoustic qualities are useful as high-resolution sound sensors.[11] Numerous other possibilities are waiting to be explored.

3. COMPARISON OF SPECTROSCOPIC TECHNIQUES

The different aspects of established spectroscopic spectral sources such as Geissler tubes, beam-gas, and beam-foil excitation will be discussed. These different sources create excited states and spectra in different ways and certain aspects of each source can be related to the beam-gel experiments that were performed. The convention of mass-per-unit-area for the materials used will be explored as a means of comparison. It is a simple relation of distance in mass/unit area = distance in length units X density.[12]

3.1. Beam-Gel

The beam-gel experiment and the theoretical parameters associated with it can now be reviewed. This will give some insight for what takes place and give an intuitive feel for what radiations can be expected from particle bombardment of a gel. For the experiments, a beam of high energy particles was directed at a mounted gel. The particle beam was either H^+ (proton), H_2^+, or H_3^+, ranging in energies from 0.25 to 1.0 MeV, giving particle velocities ranging from 4.00×10^6 to 1.70×10^7 m/sec. The density of the silicon gel used in our experiments was 1×10^{-1} g/cm^3. This, with the thickness of the thinnest gels we used as 4 mm, (Section 6.2) gives a mass-per-unit-area of 4×10^{-4} g/cm^2.

3.2. Geissler Tube

A Geissler tube creates the spectra from excited gases. It is a glass tube containing a relatively pure gas with electrodes at either side. An AC or a DC voltage applied across the electrodes causes an electric arc, and then a gas discharge. The atoms of the gas are excited by many random collisions with electrons. These collisions place them in various energy levels which ultimately decay emitting photons. The resulting spectra contain wavelengths corresponding to the different transition energies, which are characteristic of the particular atom. Although the Geissler tube is a spectroscopic device widely used, it was primarily used for calibrations in our experiments.

3.3. Beam-Gas

The gas in a beam-gas experiment, when gas in a target chamber is being bombarded with a particle, is similar to the excited condition that occurs in a Geissler tube. In the beam-gas case the "exciting current" is supplied via the accelerated particles, which collide with the gas atoms, creating excitation and ultimately spectra of the gas inside the chamber.[13] One significant difference between Geissler tube and beam-gas spectroscopy is that in a Geissler tube there is a Maxwellian distribution of electron energies,

where as in beam-gas, all the protons have the same energy (δ-function distribution).

The density of air at 1 atm is 1.2×10^{-3} g/cm^3. Gas has a linear relationship between density and pressure so a gas conversion constant of 1.18×10^{-5} g/N·cm can be used to find the density at different pressures and vise versa. To obtain the same density as the aerogel, the pressure in the target chamber would need to be 8.4×10^6 N/m^2 or 6.4×10^4 torr. For the same mass-per-unit-area as the gel, considering the diameter of the target chamber (7 cm) as the air's thickness, a pressure of 4.8×10^5 N/m^2 or 3.6×10^3 torr would be needed. Note that these pressures are so great that the interaction of the atoms would Stark shift and quench any light that may have been present. Gas excitation experiments require a pressure high enough to create just a minimum number of collisions to see the radiation.

3.4. Beam-Foil

Beam-foil spectra are created when the accelerated ions produced in the accelerator are abruptly excited (10^{-14} sec) by going through a thin excitation foil ($\approx$ 1000Å). This collision creates beam ions of different charge states, or excited neutral atoms if the beam ions extract an electron from the foil. After the foil, the excited states of the beam particles decay creating the spectrum characteristic of the particular transition. In addition the life-time of a

single transition can be studied by measuring the spectral intensity as a function of distance downstream from the foil.[14,15] The foil is solid and can not be easily viewed internally. The light from the interaction comes from the beam downstream from the foil.

The density of silicon is 2.33 g/cm^3. A foil 0.1 μm thick with that density would have a mass-per-unit-area of $2.33x10^{-7}$ g/cm^2. Thus, even though the density of the foil is 23 times greater than that of the gel, the mass-per-unit-area seen by the particle beam is 1700 times smaller then the gel's because of the thicknesses of the targets. To achieve the same mass-per-unit-area, the foil would need to be 1/23 the thickness of the gel, or the gel would need to be 23 times as thick as the foil.

The Geissler tube, beam-gas interaction, and the beam-gel targets are all transparent and the spectra are emitted from inside the source. The gel is a solid, so it may be possible to get information from observations downstream, as in the beam-foil experiments. Setting up a beam-gas experiments to have the same mass-per-unit-area as the beam-gel is essentially impossible and would probably yield minimal data due to the high pressure required. Nevertheless it is interesting to compare the thickness of the gel to the thickness of the foil. The gel excitor might be a good way to study the internal effects of a beam

traveling though a solid like a foil. Now we discuss what the spectra from the excited gel might look like.

4. COMPARISON OF SPECTRAL SOURCES

We will compare the origins of spectra from the following sources - ionization, atomic excitation, black body, luminescence, Bremsstrahlung, Cherenkov, and synchrotron. The physical process for creating these radiations and the relevant equations associated with them might give some clues to the source of the aerogel spectra.

The spectra from different types of light sources have unique characteristics, but basically they can be characterized as: lines and continua, or a combination of the two. Spectral lines are large intensity peaks at particular wavelengths associated with a single atomic transition. A continuum consists of a large number of continuous wavelengths and, while being very broad, can be characterized by its peak wavelength. Spectral lines and a continuum can appear in the same spectra.

4.1. Ionization

Ionization can occur by the actual collision of the incident and target molecules, but the probability of such an interaction is very small. Most interactions occur though Coulomb's force at a distance. Rutherford derived the differential angular cross-section for the interaction of a incident particle and a target nucleus (Equation 4.1). He assumed the nuclear model with the target nucleus fixed. Both the particle and the nucleus are treated as point-like

charges with only the Coulomb force acting between them. The particle and nucleus elastically scatter, according to classical mechanics.[16]

$$\frac{\partial\sigma}{\partial\Omega} = \left(\frac{Z\cdot z\cdot e^2}{16\cdot\pi\cdot\varepsilon_o\cdot T}\right)^2\cdot\operatorname{cosec}^4(\theta/2) \qquad (4.1)$$

Ze = target nucleus charge	(C)
ze = incident particle charge	(C)
θ = angle of scatter	
ε_o = permittivity of free space	($C^2/N\cdot m^2$)
T = kinetic energy	(J)

In terms of the particles momentum and velocity Rutherford's differential angular cross-section can be written as equation 4.2.[17]

$$\frac{\partial\sigma}{\partial\Omega} = \left(\frac{z\cdot\alpha\cdot\hbar\cdot c}{2\cdot p\cdot v}\right)^2\cdot\operatorname{cosec}^4(\theta/2) \qquad (4.2)$$

α = fine structure constant	
$\hbar$ = Planck's constant over $2\cdot\pi$	(J·sec)
c = speed of light	(m/sec)
p = momentum of incident particle	(kg·m/sec)
v = velocity of incident particle	(m/sec)

Mott extended Rutherford's differential angular cross-section to account for incident electrons that might be relativistic in nature (Equation 4.3).[18]

$$\frac{\partial\sigma}{\partial\Omega} = \left(\frac{z\cdot\alpha\cdot\hbar\cdot c}{2\cdot p\cdot v}\right)^2\cdot\operatorname{cosec}^4(\theta/2)\cdot\left[1 - \frac{v^2}{c^2}\cdot\sin^2(\theta/2)\right] \qquad (4.3)$$

p = momentum of electron	(kg·m/sec)
v = velocity of electron	(m/sec)

Using Mott's equation and changing the frame from the electron incident on a nucleus to a nucleus incident on a electron it is possible to derive the Bethe-Bloch equation. The Bethe-Bloch equation pertains to the deceleration of

arbitrarily charged particles due to interactions with the electrons of the target molecules. Equation 4.4 gives the loss of kinetic energy per distance traveled.[19]

$$-\frac{dT}{dx} = \frac{n \cdot Z \cdot z^2 \cdot 4 \cdot \pi \cdot \alpha^2 \cdot \hbar^2}{\beta^2} \cdot \left[\ln\left(\frac{2 \cdot m \cdot c^2 \cdot \beta^2}{I \cdot (1-\beta^2)} \right) - \beta^2 \right] \qquad (4.4)$$

n = atoms per volume ($\#/m^3$)
m = electron mass (Kg)
I = mean excitation potential, $16 \cdot Z^{0.9}$ (J)

The energy of the particle is absorbed by the target material's electrons, creating excitation, or, if the energy of the incident particle is great enough, ionization. The ionized electrons can cause further excitation through collisions. At energies below the ionization threshold the electrons will lose energy in collisions with atoms of the target material, causing thermal excitation of the absorbing material. This heating of the material creates electromagnetic radiation. The structure of some transparent materials can luminesce in the visible or near-visible part of the spectrum: such materials are called scintillators.[20]

4.1.1. Atomic Excitation

If the electrons are from unbound atoms, such as the particle beam in beam-foil and the gas in beam-gas, the electrons of the atoms can be excited to discrete allowed energy levels. Once there, they can be further excited or they can decay back to their ground state. When the

electrons decay, they emit energy in the form of photons. These can be detected. Since there are quantized energy states, and only certain transitions between them are allowed, the spectra are made up of distinct spectral lines. These lines can classify emitting sources because of the relationship between energy, E, and wavelength, $E_{if} = \Delta E_{if} = E_f - E_i = (h \cdot c)/\lambda_{if}$. Here h is Planck's constant 6.626×10^{-34} J·sec, c is the speed of light 2.998×10^{8} m/sec, and λ is the wavelength of the spectral line in meters. The combination of these spectral lines is unique for every atom, and their wavelengths can identify their source.

4.1.2. Black Body Radiation

If the electrons are from atoms in a solid, the electrons can vibrate due to the thermal excitation. These vibrations cause the solid to emit electromagnetic radiation in the form of a continuum. A black body is defined to have an absorption power of one and its spectrum is independent of the physical or chemical properties of the material. A black body is a perfect radiator, meaning its radiation is homogeneous, isotropic, and unpolarized. Kirchhoff first stated that any body in thermal equilibrium with the radiation has a ratio of emissivity to absorption power that depends only on the frequency of the light emitted and the absolute temperature of the body.[21]

W. Wien studied the spectral energy density, using only thermodynamics and Maxwell's laws, and deduced his exponential law $u(f,T) = A \cdot f^3 \cdot e^{-\beta \cdot f/T}$, where A and β are constants.[22] Planck interpolated between Wien's exponential law and an energy density proportional to temperature to derive his formula for black body radiation (Equation 4.5). Planck's equation matched the experimental data from black body radiation.[23]

$$u(f,T) = \frac{8 \cdot \pi \cdot h \cdot f^3}{c^3} \cdot \frac{1}{(e^{h \cdot f/k \cdot T} - 1)} \qquad (J \cdot sec/m^3) \quad (4.5)$$

h = Plank's constant	(J·sec)
k = Boltzmann's constant	(J/°K)
c = speed of light	(m/sec)
f = frequency	(Hz)
T = temperature	(°K)

As the temperature of the black body rises, the wavelength of the peak intensity moves toward the blue spectral region (shorter λ). The entire spectral distribution from x-ray to radio wave for a given temperature can be totally characterized by giving the wavelength of the peak intensity. Wien's displacement law gives an accurate behavior for λ_{max} (Equation 4.6).[24]

$$\lambda_{max} = A/T \qquad (m) \qquad (4.6)$$

$A = 2.898 \times 10^{-3}$	(m·°K)
T = temperature	(°K)

4.1.3. Luminescence

If the electrons are from atoms of a special transparent solid, they may luminesce. When atoms bond to

form a solid, the atoms' discrete energy levels form energy bands. These bands create new energy levels that appear as metastable states that the electrons can transit to, giving rise to emitted photons of different energies, i.e. a continuum.[25]

The occurrence of excited states below the normal excited state allows for the classification of luminescence as fluorescence or phosphorescence. If the electron returns to the ground state by emitting radiation not corresponding to the initial absorption (β-process), then it is fluorescence. If the electron goes to a lower metastable state and then returns to the initial excited state to decay emitting radiation corresponding to the initial absorption (α-process), then it is phosphorescence. Fluorescence is temperature independent, where as phosphorescence is sensitive to temperature. Fluorescence usually has a greater time lag than phosphorescence, but the temperature dependence can affect that greatly. With fluorescence, there is no separation of the electron from the ion, keeping the same spin the entire time. Phosphorescence is a separation of the electron from the ion, with a change in the electron spin. Both phenomena can occur in the same substance with the ratio of intensities dependent on numerous factors.[26] Fluorescence tends to be prevalent in

smaller atoms, whereas phosphorescence is more prevalent in the larger atoms.[27]

4.2. Bremsstrahlung Radiation

Bremsstrahlung radiation is a form of electromagnetic radiation similar to that of ionization. It too is a loss of kinetic energy per unit distance but here the particles are scattered and decelerated by the electric field of a nucleus near its path. It is also known as "braking radiation". Electrons have a very small mass, so they are easily deflected by the nucleus's charge. Equation 4.7 gives the electron kinetic energy lost per distance traveled in the material.

$$-\frac{dT}{dx} = \frac{4 \cdot n \cdot Z^2 \cdot \alpha^3 \cdot \hbar^2 \cdot T}{m^2 \cdot c^2} \cdot \ln\left(\frac{183}{Z^{1/3}}\right) \quad \text{(eV/m)} \qquad (4.7)$$

n	= atoms per volume	$(\#/m^3)$
Z	= atomic number of material	
α	= fine structure constant	
$\hbar$	= Planck's constant over $2 \cdot \pi$	$(J \cdot sec)$
c	= speed of light	(m/sec)
T	= kinetic energy	(eV)
m	= electron mass	(Kg)

The spectrum from the Bremsstrahlung radiation is also a continuum, usually peaking in the x-ray spectral region.[28]

4.3. Cherenkov Radiation

Cherenkov radiation is created by a charged particle traveling through a material with a speed greater than the phase velocity of light in that material. When that

criterion is met, the particle creates a coherent wave of light that travels in the form of a cone with an angle defined by $\varphi = \Pi/2 - \theta$, where θ is the angle defined by equation 4.8.

$$\cos\theta = \frac{c}{n \cdot v} \qquad (4.8)$$

c = speed of light (m/sec)
n = index of refraction
v = particle velocity (m/sec)

To get Cherenkov radiation, we must have v>c/n. If this criterion is not fulfilled, then there will be no real values for θ. Cherenkov radiation is essentially a continuum light source.[29]

4.4. Synchrotron Radiation

Synchrotron radiation is a form of electromagnetic radiation similar to that of Bremsstrahlung radiation. It is formed by the centripetal acceleration of charged particles, such as electrons, in a magnetic field traveling at speeds close to that of light. Due to the very high velocities, relativistic effects cause the usual dipole emission pattern to be strongly peaked in the momentary forward flight direction, causing linearly polarized radiation. The power produced by the peak is given by equation 4.9.

$$P = \frac{2 \cdot c \cdot E^4 \cdot r_o}{3 \cdot R^2 \cdot (m_o \cdot c^2)^3} \qquad \text{(Watts)} \qquad (4.9)$$

c = speed of light (m/sec)
E = electron energy (J)
r_o = radius of particle (m)

R = radius of curvature (m)
m_o = mass of particle (kg)

In equation 4.9, the radius of the particle is given by $r_o = q^2/4 \cdot \pi \cdot \varepsilon_o \cdot m_0 \cdot c^2$, q is the charge in coulombs, and ε_o, is the permittivity of free space, 8.854×10^{-12} $C^2/N \cdot m^2$.[30] The radius of the particle is used as the distance separating the poles of the dipole. The peak intensity (constant in the flight direction) continuously changes direction with the moving electron, causing the intensity to sweep over the detector in a very short time. Fluctuations in the energy and the orbit's radius cause the frequency distribution to be smeared out into a continuum. This continuum has a characteristic wavelength given by:

$$\lambda_c = \frac{5.6 \cdot R}{E^3} \quad (\text{Å}) \qquad (4.10)$$

E = particle energy (GeV)
R = radius of curvature (m)

The unit conversions are accounted for in the equations constant.[31]

5. EXPERIMENTAL METHOD AND TECHNIQUES

The experimental setup used to study radiation from the particle excited gel has eight components. These are (1) the ion accelerator, (2) the bending magnet, (3) the beam line, (4) the target chamber, (5) the external optics, (6) the spectrometer, (7) the photomultiplier tube and electronics, and (8) the data acquisition and manipulation system. Most of the experimental setup was readily available in the 2 MeV beam-foil lab, which was used to pioneer beam-foil spectroscopy at the University of Arizona. Figure 3 shows the entire set-up.

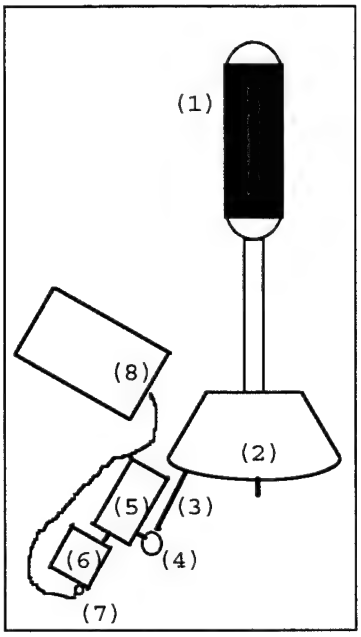

Figure 3: Set-Up

5.1. Accelerator Ion Source

The main instrument is the Model AN-2000 2 MeV Van de Graaff Accelerator built by High Voltage Engineering Corporation, Burlington, Massachusetts. It can accelerate positive ions to energies between 0.2 to 2.0 MeV. Figure 4 shows the mechanics of the accelerator. A belt driven into the high voltage (HV) hemisphere terminal at the opposite end of the accelerator extracts electrons from the inside of the terminal dome causing the build-up of a positive high voltage on the outside surface. The electrons are removed

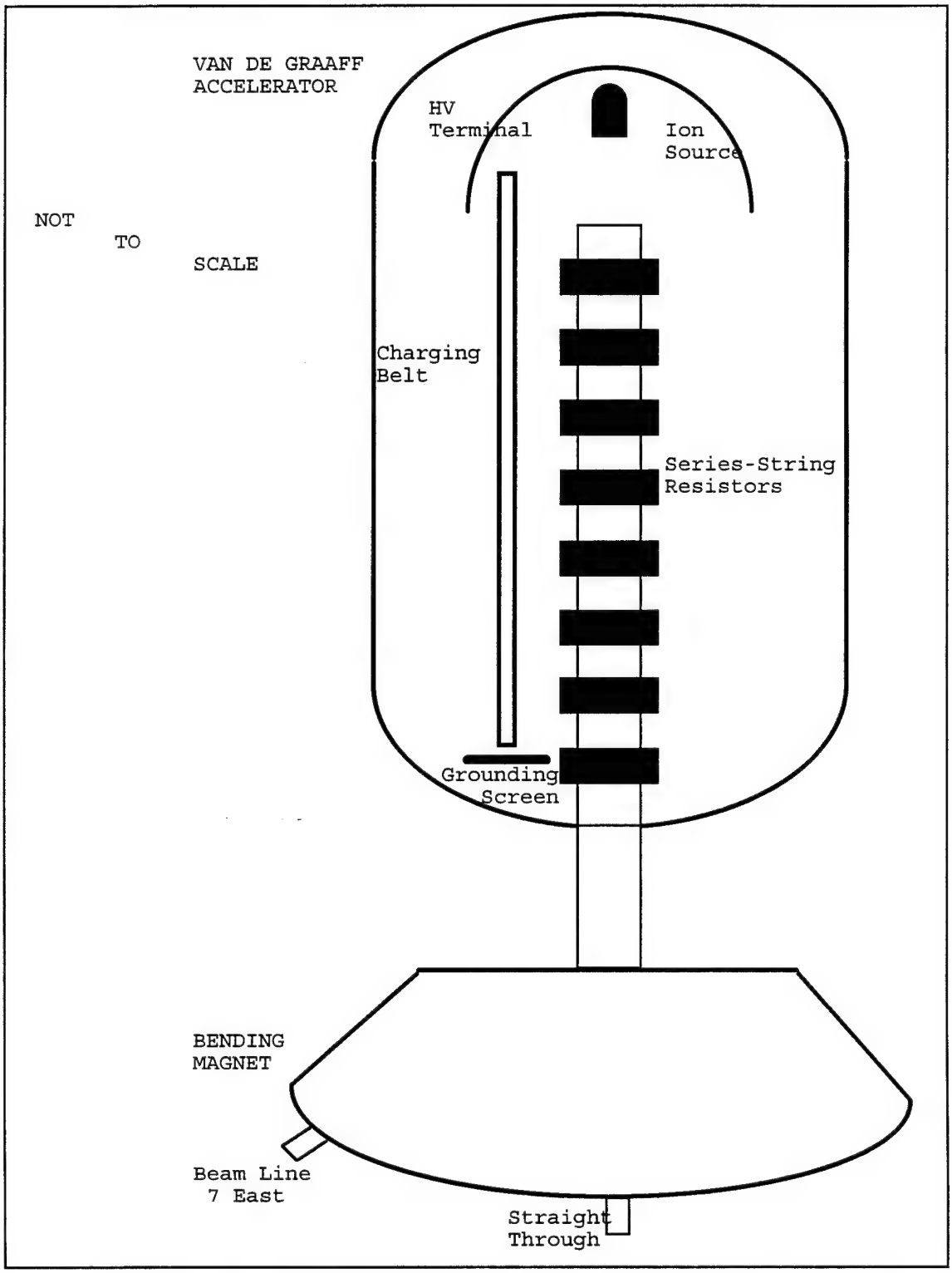

Figure 4: Accelerator and Bending Magnet

at the bottom by a grounding screen. The dome is insulated from the shell of the accelerator with a mixture of inert CO_2 and N_2 gas to prevent arcing. Inside the HV terminal, a glass ion source is filled with the gas to be accelerated. The gas is ionized by radio frequency, rf, energy, creating a plasma. A positive anode probe opposite the exit hole forces the ions out of the bottle into the accelerator tube, where it feels the repulsive strength of the positive HV terminal. This force accelerates the ion down the length of the accelerator tube to ground at the far end.[32] The highly evacuated accelerator tube connects to an external evacuated beam pipe. The high vacuum is necessary to minimize collisions between the accelerated particle and air particles in the tube. Pressures remained around 1.1×10^{-6} to 1.2×10^{-6} torr, 1.5×10^{-4} to 1.6×10^{-4} N/m^2, giving a mean free path of approximately 200 m.

5.2. Bending Magnet

After exiting the accelerator, the particle beam enters an electromagnet (See Figure 4) which deflects the beam particles into a particular beam line. The magnet separates various ion beams according to the Lorentz force (Equation 5.1).

$$F = q \cdot (v \times B) \qquad (5.1)$$

q = charge of the particle
v = velocity of the particle
B = magnetic field

Setting $F = m \cdot a$ and substituting $v^2/r = a$, the centripetal acceleration, into the equation, equation 5.2 is obtained.

$$m \cdot v = q \cdot B \cdot r \qquad (5.2)$$

r = radius of curvature

Substituting in the kinetic energy $E = \frac{1}{2} \cdot m \cdot v^2$, equation 5.3 is obtained.

$$m = \frac{B^2 \cdot q^2 \cdot r^2}{2 \cdot E} \qquad (5.3)$$

The radius of curvature for a given beam line (the seventh east beam line was used in our experiments), is constant, and the charge for all of the accelerated particles is plus one. By adjusting the energy and magnetic field, the desired beam particle can be deflected into the proper beam line. Problems arise when particles like CO^+ and N_2^+ contaminate the beam. Their masses, both approximately 28, are nearly indistinguishable, and will appear in the same particle beam.

5.3. Beam Line

The beam particles travel from the bending magnet to the target chamber via a 63.5 mm diameter, 1 m long beam pipe. Fluctuations in the energy of the accelerator cause the beam to wander. To prevent this, energy control slits are located in the beam pipe. If the energy increases, or decreases, the beam passing between the two slits will slip

left or right - creating a slit current. This sends a feedback signal into the accelerator to counteract the slit current. Thus the slits maintain a constant particle energy and this keeps the beam on target.

5.4. Target Chamber

Finally the ion beam enters the target chamber through a 15 cm aluminum plug with a 6 mm hole through the central axis. The chamber has quartz windows on both sides, perpendicular to the beam path. The chamber has a removable top. The beam terminates in a Faraday cup which collects the beam current entering the chamber. The Faraday cup current is read by a RCA Ultra Sensitive DC Microammeter WV-84C. Diffusion pumps in the beam lines and target chamber keep a constant high vacuum around $2x10^{-5}$ torr or $2.67x10^{-3}$ N/m^2.

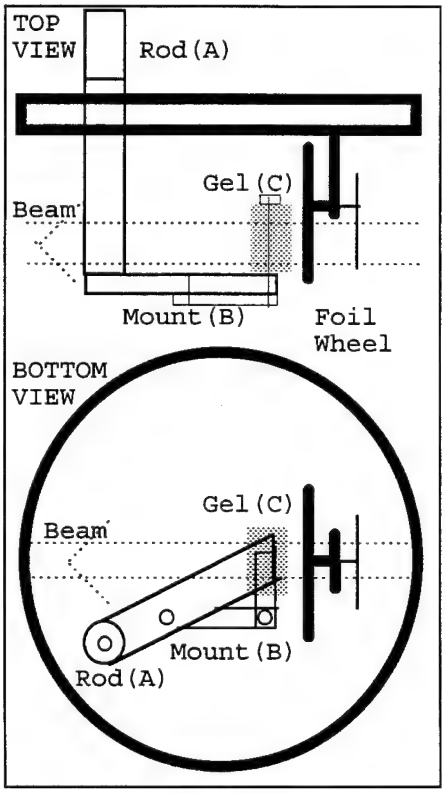

Figure 5: Target Chamber

The innards of the target chamber are shown in Figure 5. A wheel mount, mechanically connected to the outside of the chamber, can rotate foils in and out the beam path. An aluminum rod (A) passes through the top and connects to a Plexiglas mount (B) that holds the aerogel

(C). The mount is a thin piece of Plexiglas extending from the rod with an additional piece of Plexiglas on a screw that can be adjusted to clamp the gel firmly. The gel can be rotated in and out of the beam path by turning the rod. The pressure inside the chamber is read by a National Research Corporation's, Model 803, 115 V, 60 Hz, 2 W pressure gauge located on the magnet side of the aluminum plug.

5.5. External Optics

Light essentially normal to the beam in the target chamber is focused on to the monochromator entrance slit by a parabolic mirror (See Figure 6). The mirror could be rotated about its axis point A to the right or left to collect light from different points P on the beam by a calibrated micrometer screw. This swept the observation point of the entrance slit along the beam in the target chamber. The point P could be moved 25 mm along the beam. It started at the foil holder, went across the gel, and to the region behind the gel. A one-micron displacement of the mirror arm translated to a lateral movement of 0.221 mm inside the target chamber. To get continuous sweeps along the beam a Hurst MFG Corporation, Model PC DA, 115 volt, 60 Hz motor turned the micrometer. The center of the beam was located at the focal point of the parabolic mirror.

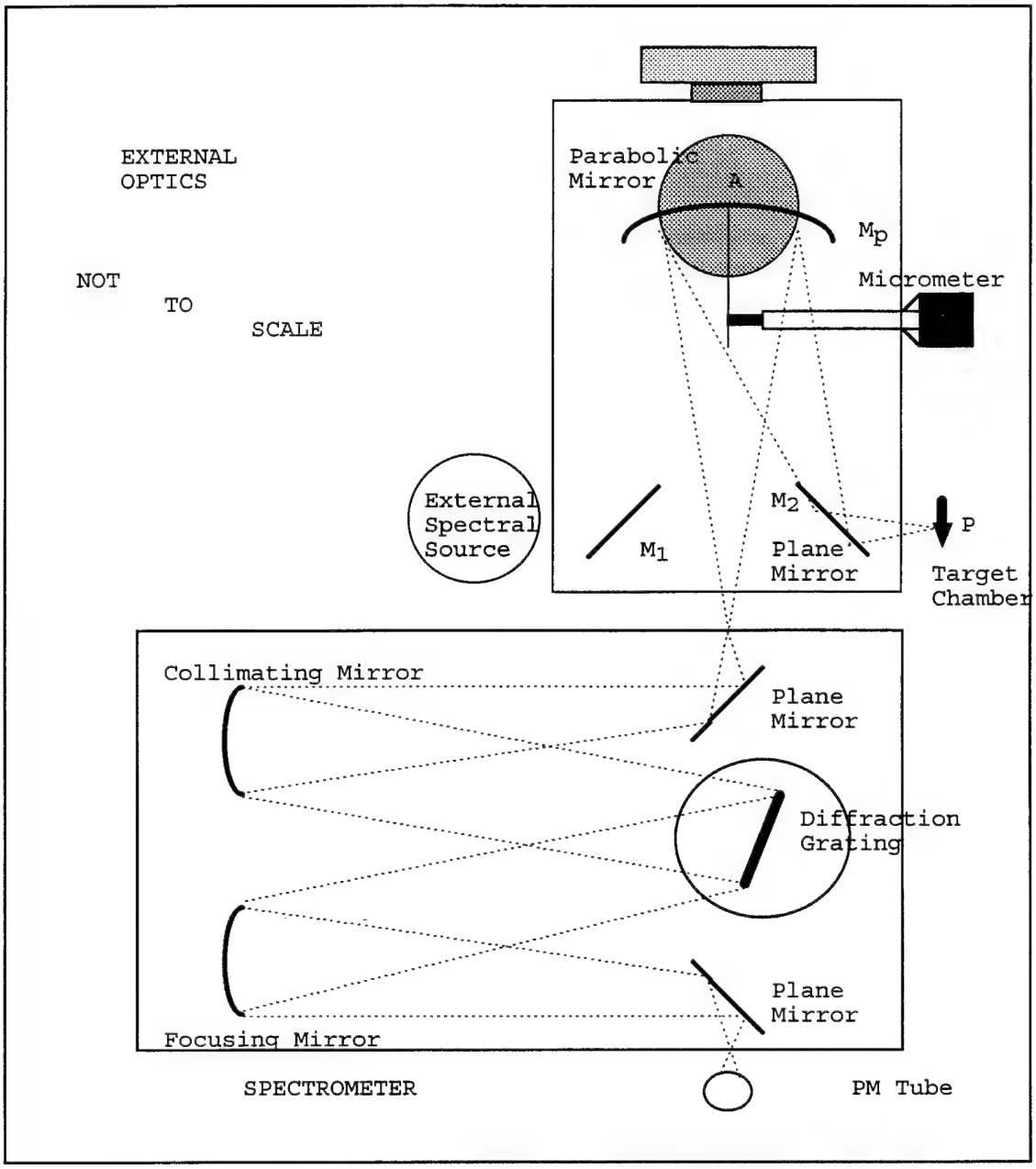

Figure 6: External Optics and Spectrometer

5.6. Spectrometer

A Heath EU-700/E Scanning Monochromator extracted the spectral information from the light emitted by the beam-gel. It is a single-pass Czerny-Turner with folding mirrors that

give the entrance and exit slits a common optical axis (see Figure 6). It has an aperture ratio of f/6.8 at 2000 Å with a focal length of 350 mm. It has a resolution of 1 Å and a line-profile half width less than 0.5 Å at 3 mm slit height. It can scan wavelengths from λ1900 to 10000 Å with nine different scan settings from 0.05 to 20 Å/sec, or an increasing or decreasing slew rate of 5400 Å/min. It has a reciprocal dispersion of 20 Å/mm with an 1180 lines/mm grating. The full dimensions of the grating are 48 mm x 48 mm with 1180 lines/mm. The slit widths range from 5 to 2000 μm and slit heights from 3 to 15 mm. The wavelength scan is a sine bar and precision leadscrew assembly run by 0.1 Å/step stepper motor. The mirrors are aluminized first-surface mirrors with MgF_2 overcoating corrected to one-fourth wavelength of the Hg green line at λ5461 Å. The collimating and focusing mirrors are 55 mm in diameter, parabolic with a focal length of 350 mm. The folding mirrors are 25 mm x 35 mm plane mirrors.[33]

The spectrometer transfers the exact image of the entrance slit to the exit slit. The light enters the spectrometer through the entrance slit, which is one focal length from the collimating mirror. The light reflects from the folding mirror into the collimating mirror. The collimating mirror reflects parallel light on to the

diffraction grating. The diffraction grating separates the spectral lines according to the reciprocal dispersion. The grating is turned by the stepping motor with the leadscrew and the sine-bar, which converts the linear motion to sinusoidally-varying angular motion. The parallel light reflecting from the grating hits the focusing mirror, which then reflects it to the second folding mirror which focuses it onto the exit slit. As the grating rotates, different wavelengths are aligned with the exit slit. The radiation passes through the slit and is collected by a photomultiplier used as the photon detector.

5.7. Photomultiplier Tube

The detector was a RCA Model 1P21-2 photomultiplier (PM) tube, number 2-T06950A, with the following properties. The maximum permitted operating voltage is negative 900 VDC. Exceeding this voltage limit can permanently damage the tube causing internal electrical breakdown, leading to excessive noise readings. Any signal obtained while the tube is totally dark is known as dark current. It is caused by thermal excitation of the photocathode and cosmic rays. Thermal excitation of the photocathode causes spontaneous electron emissions. The cosmic rays generate Cherenkov radiation when passing through the glass casing of the tube. The resulting radiation is then registered on the photocathode. The dark current at the highest operating

voltage is 5.0×10^{-10} A. The maximum allowable current from the PM tube is 1.8×10^{-6} A. The PM tube is encased in a Borosilicate glass case. It operates in the visible wavelength range, λ3000 to 6500 Å, with a maximum sensitivity at a wavelength of λ4000 Å. The cathode is rectangular, with dimensions of 0.2 mm x 0.61 mm.

A Keithley Instrument 240 A High Voltage Supply powered the PM tube. The optimum operating high voltage for both the noise to signal ratio along with the best statistics was 860+10 VDC. Curiously, this HV setting was different from the 870 VDC setting, a result of the internal configuration of the high voltage source. At this voltage the PM tube dark current was 4.0×10^{-10} A.

A PM tube is a photon detector with several dynodes between the cathode and anode. The desired photocathode shape is based on the shape of the photon beam that enters the PM tube. Since the monochromator entrance and exit slits are rectangles, the photocathode is also a rectangle. A photon entering the PM tube strikes a photocathode which has a set work function. The photon energy must be greater than the work function to eject an electron. An electron ejected is slightly accelerated and hits the first of a series of dynodes at different potentials, resulting in a "magnification" of the number of electrons in the pulse. The resulting electron gain is N^d, where N is the average number

of electrons emitted per dynode and d is the number of dynodes (9 in our PM tube). The single final current pulse is not infinitely narrow, but has a width and distinct shape. The PM tube pulses are characterized by their height, length, and half width. The pulse leaving the PM tube can then be directed toward other instruments for further analysis.

5.8. Data Acquisition

The PM tube signal can be sent to different instruments for storage and data analysis. Two different configurations were used in the experiments performed.

To measure the PM tube current, the signal from the PM tube went to a Keithley Instrument 414S Picoammeter, with a range from $1x10^{-11}$ to 0.01 A. A one volt for full scale output was fed to a Fischer Scientific Recordall series strip chart. The chart was set at one volt full scale to accommodate the one volt output from the picoammeter. Several chart speeds (cm/min) were used to adjust the wavelength scale of the data. The strip chart could be replaced by a computer. In this case the output from the picoammeter went into a Hewlett Packard 34401 A Multimeter attached via a GP1B interface to an IBM personal computer. The data were then stored on floppy disks that could be analyzed with standard spectral analysis programs.

Another data taking configuration incorporates an amplifier, multi-channel analyzer, and a strip chart. The PM tube signal goes directly to the amplifier, and then to a Tennelic TC 214 Linear Amplifier and Single Channel Analyzer. The amplifier was optimized at gain levels 32x8. The signal from the amplifier was then fed into a Tracer Northern NS-575A Digital Signal Analyzer, which counts the number of pulses that arrive in a certain period of time and stores them in a single channel. The multi-channel analyzer is much more sensitive than the picoammeter and has a faster time response. Unlike the picoammeter, the multi-channel analyzer stores the counts for every pulse in memory which then can be transferred to a strip chart or plotter.

5.9. Other Experimental Equipment

A Staco Energy Products Co., Input 120 V, 50/60 Hz; Output 0-120/140 V, 10 A, 1.4 kVA, variable autotransformer was used with the Geissler tubes and the blackbody source. To get the blackbody radiation curves, a Model A2CO, 120 V, 7.5 W light source was used. An Ultra-Violet Products Inc., Model SCT-1, 115 V, 60 Hz, 0.48 A, Pen Ray Power Supply was used to power a mercury lamp for the gel luminescence test.

6. EXPERIMENTAL PROCEDURE

6.1. Preliminary Data

The spectra from various known gaseous elements in Geissler tubes were studied first. Both monatomic and diatomic gases were studied to determine the main spectral differences. The parabolic mirror in the external optics was adjusted to collect light from the Geissler tubes. The spectra were taken from λ3500 to 7000 Å at a scan rate of 10 Å/sec. The intensity scale for each scan was adjusted to keep the most intense line on scale. The same procedure was used to get spectral scans of the black body source. Different black body voltage (current) settings were directly related to different black body temperatures. At a maximum of 120 V the temperature was 2160^{o}K. Proper lamp adjustment and a diffuse glass placed in front of the entrance slit were used to adjust the intensity of the beam entering the spectrometer. The black body source was then replaced by a mercury lamp shining on a gel on a Plexiglas platform to evaluate changes in luminescence.

6.2. Gel Preparation

The gel samples used in the experiments were cut from 50 x 40 x 13 mm gel blocks donated by Arlon J. Hunt. A razor blade on a mirror was used to cut the front incident surface, attempting to get it as smooth and square as possible. Due to the delicate structure of the gel, 4 mm

was the thinnest gel produced with regular success. Gels as thick as 10 to 12 mm were used in some of the experiments.

The gel was then carefully placed on the target chamber Plexiglas mount. The top mount support was lightly tightened to secure, yet not fracture, the gel. The gel was adjusted so the front surface area was normal to the incident particle beam and nearly perpendicular to the external optics when the rod was turned into the beam path.

Once the gel was securely fastened to the mount, the target chamber top was reattached to the chamber. The chamber was then evacuated and the gel was allowed to degas.

6.3. Gel Experiments

Wavelength scans of the particle-excited gel were made to determine what spectral lines or continua would appear. For the wavelength scans, the parabolic mirror in the external optics was turned to observe the beam (Mirror M_1). at the desired position in the target chamber. The positions corresponded to the different areas in figure 7 in

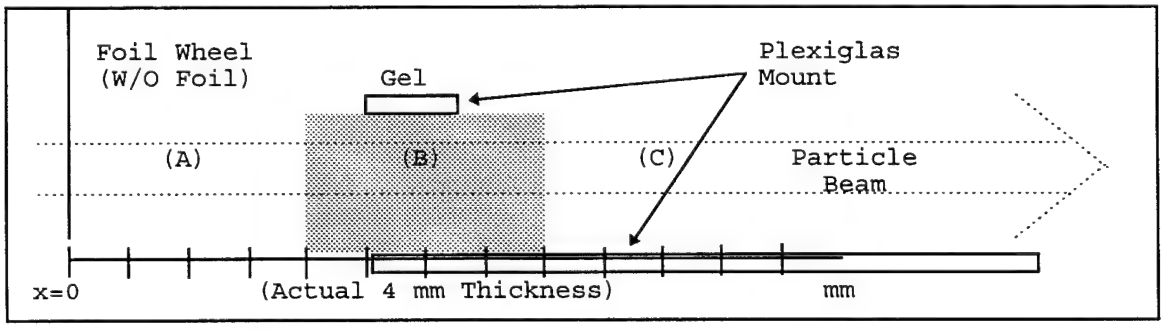

Figure 7: Location of Gel Observations

relation to the gel: (A) in front, (B) inside, and (C) behind. Spectra were taken from λ3500 to 7000 Å at a scan rate of 10 Å/sec.

Beam-gas spectral scans were performed in the three observation areas in relation to the gel. The pressure was varied along with the particle energy to see the effect on the spectra. Beam-gel spectral scans were performed in the same manner as a function of observation points and gas pressure. Three hydrogen particle beams: H^+ (protons), H_2^+, and H_3^+ were used to bombard the gel. In the beam-gas and beam-gel experiments the gas pressure was varied from $2x10^{-5}$ to $1.2x10^{-4}$ torr, or $2.7x10^{-3}$ to $1.6x10^{-2}$ N/m^2. Spectral scans were also taken of beam excited quartz.

To get a spatial intensity scan at a fixed wavelength, the motor attached to the micrometer swept the observation point P over the length of the gel from area A, in front of the gel, to area C, behind the gel. Different energies were used to show how the particle beam penetrated the gel. Gels of different thickness were used and the scan wavelengths were varied.

The gel was found to have an instantaneous excitation peak when initially subjected to the particle beam. For analysis of the time decay related to the initial excitation of the gel, the signal from the PM tube was sent to an amplifier and multi-channel analyzer. The parabolic mirror

was aligned so that the observation point P was receiving light from the upstream face of the gel. The valve between the target chamber and the beam pipe was periodically opened and closed manually.

7. DATA

The following figures show the data from our experiments. Although the picoammeter was adjusted during the acquisition to keep the maximum peaks on scale, all figures were normalized for a peak intensity of one. Figures 8, 10, 11, 14, 15, and 16 were individually normalized to their peak value. The noise in Figure 9 was normalized to observe the luminescence better. Figures 12 and 13 were normalized to their respective figure b to compare the wavelength intensities. The wavelengths shown are the accepted published values or empirical values obtained during repeated experiments.

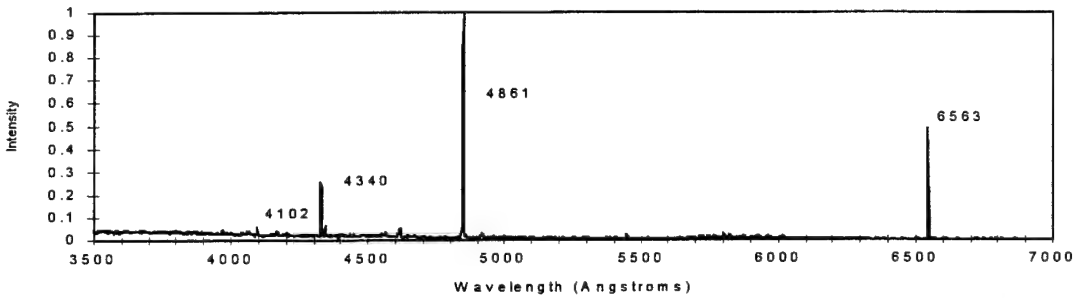

Figure 8a: Spectrum of a hydrogen Geissler tube at 55 VDC.

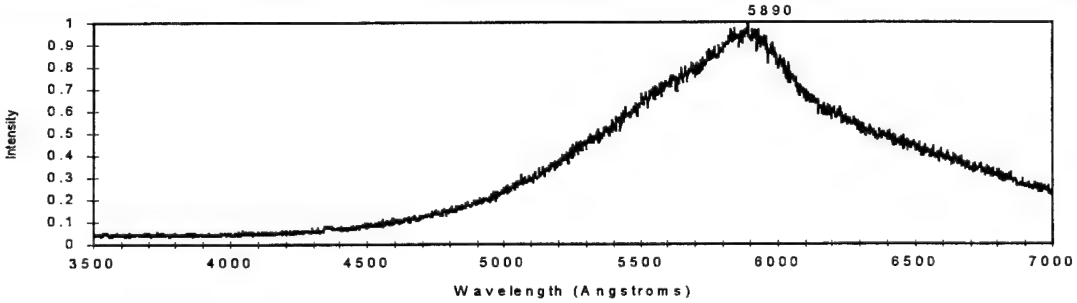

Figure 8b: Spectrum of a blackbody lamp at 24 VDC.
A calibrated temperature of 650 K.

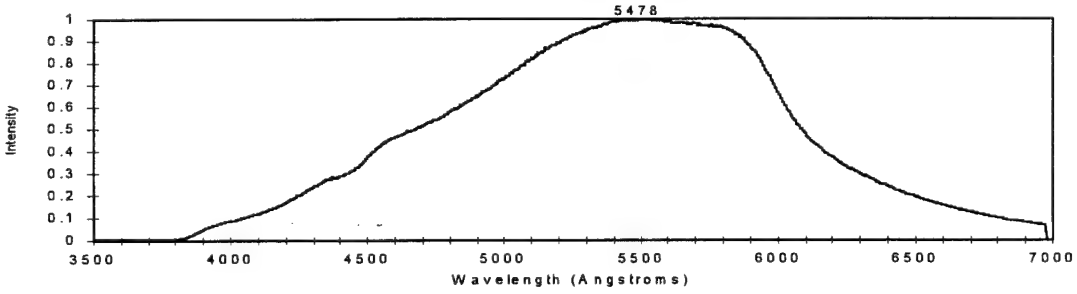

Figure 8c: Spectrum of a blackbody lamp at 120 VDC.
A calibrated temperature of 2160 K.

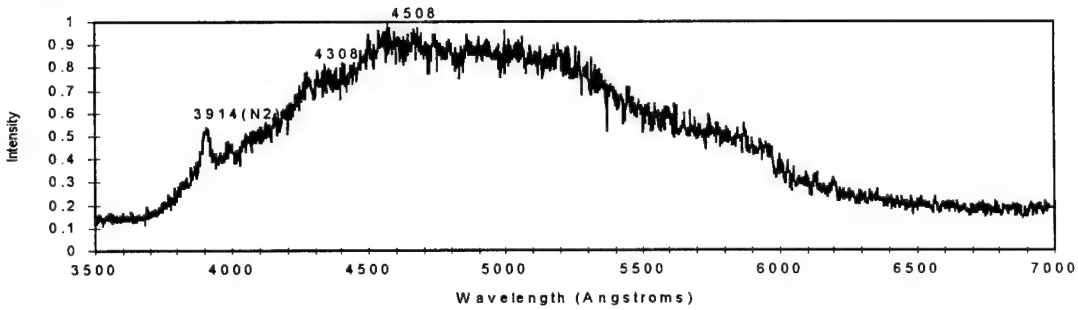

Figure 8d: Spectrum of a 5E-7 A, 0.5 MeV H3+ excited gel (P=1.2E-4 torr)
observed 1 mm inside the gel (Area B).

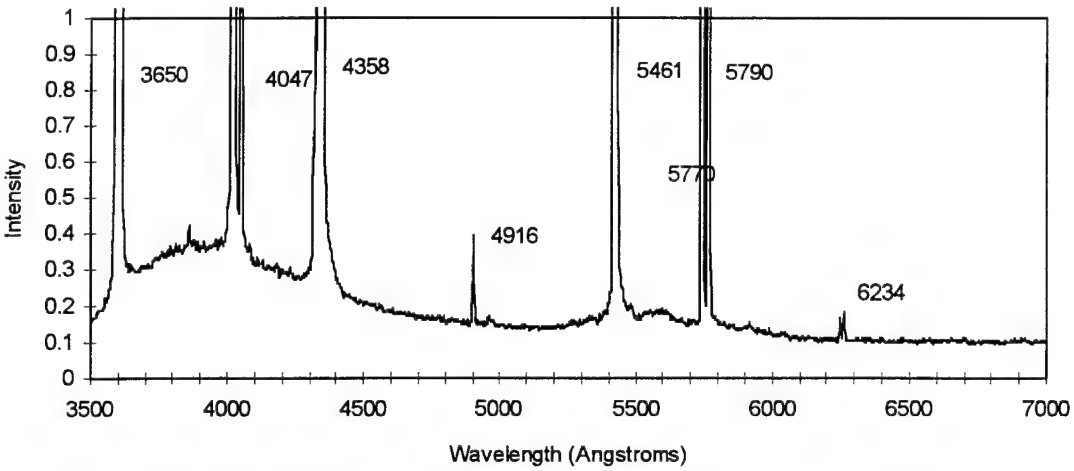

Figure 9a: Spectrum of Plexiglas plate illuminated by a mercury lamp.

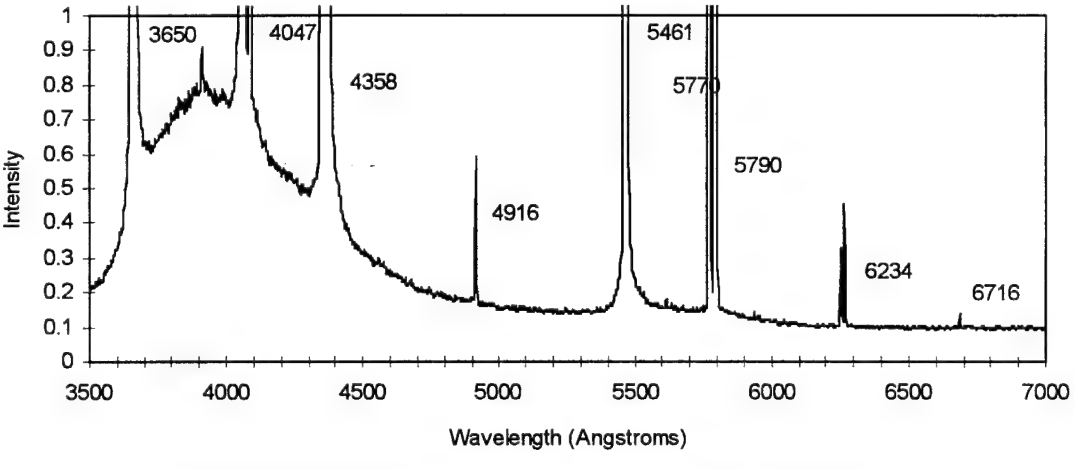

Figure 9b: Spectrum of a gel on a Plexiglas plate illuminated by a mercury lamp.

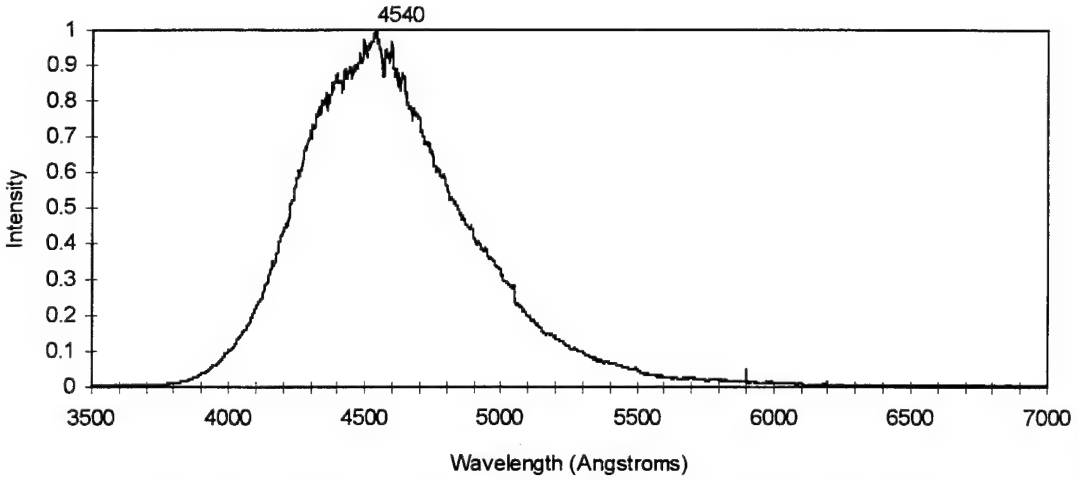

Figure 10a: Spectrum of a 5E-7 A, 0.5 MeV H3+ excited quartz plate (P=1E-5 torr) 45 degrees to the incident beam and line-of-sight.

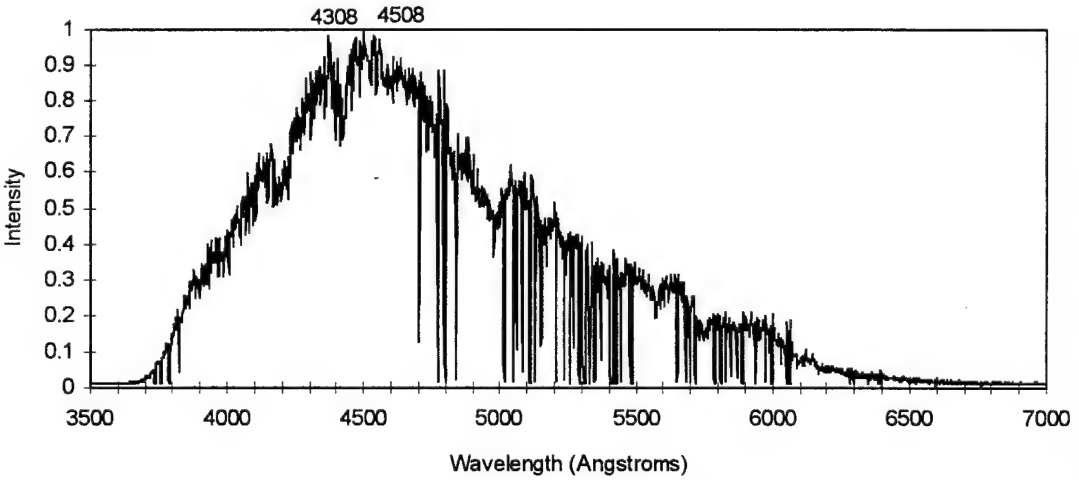

Figure 10b: Spectrum of a 6E-7 A, 0.5 MeV H3+ excited gel (P=1E-5 torr) 45 degrees to the incident beam and line-of-sight.

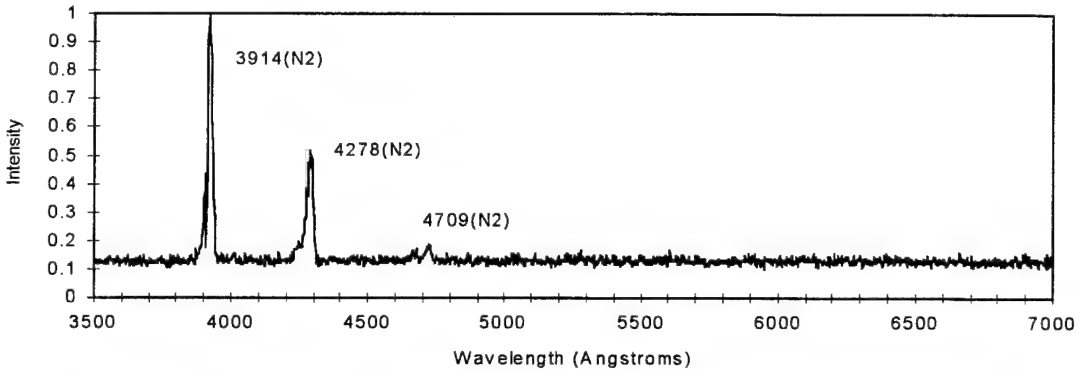

Figure 11a: Spectrum of a 4.5E-7 A, 0.5 MeV H3+ excited air (P=1.2E-4 torr) observed 3 mm downstream from the foil wheel w/o the gel (Area A).

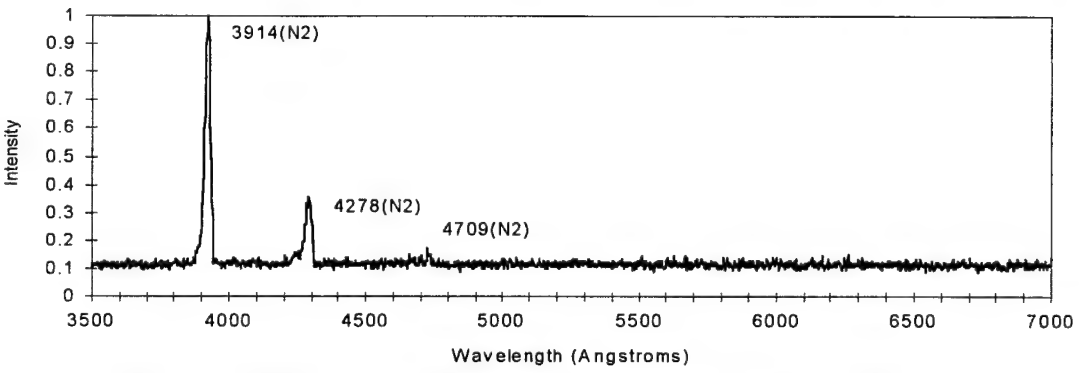

Figure 11b: Spectrum of a 4.5E-7 A, 0.5 MeV H3+ excited air (P=1.2E-4 torr) observed 5 mm downstream from the foil wheel w/o the gel (Area B).

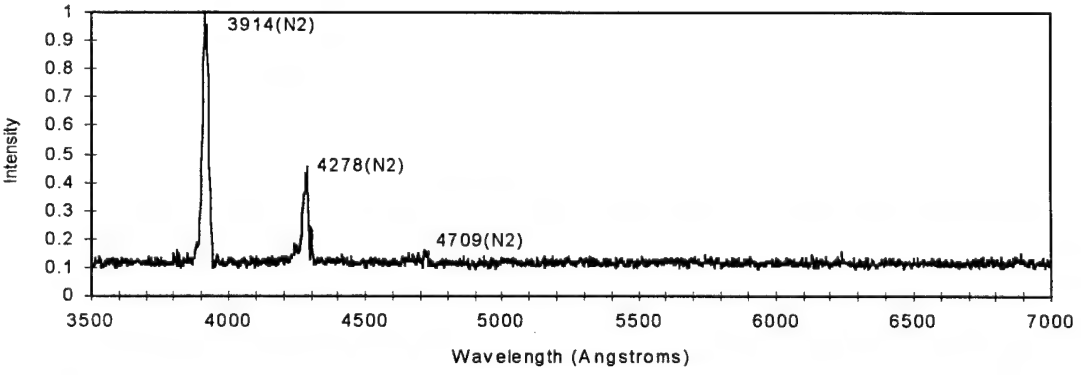

Figure 11c: Spectrum of a 4.5E-7 A, 0.5 MeV H3+ excited air (P=1.2E-4 torr) observed 10 mm downstream from the foil wheel w/o the gel (Area C).

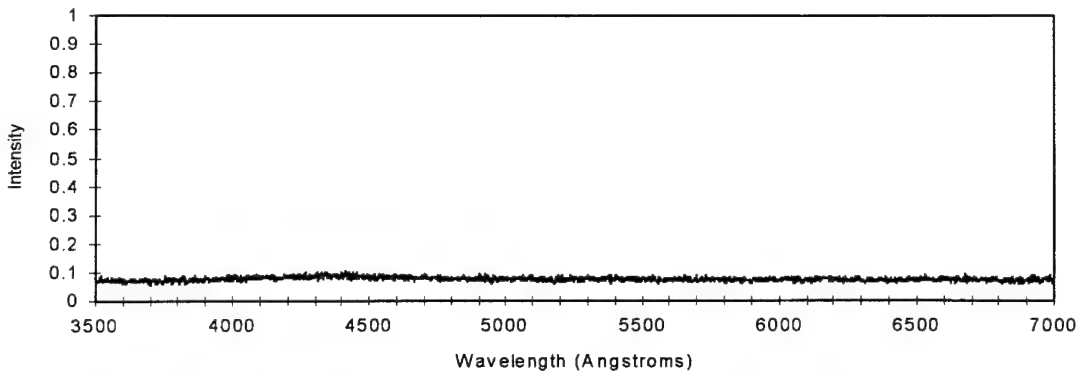

Figure 12a: Spectrum of an 8E-7 A, 0.5 MeV H3+ excited gel (P=2E-5 torr) observed 1 mm upstream from the upstream surface of the gel (Area A).

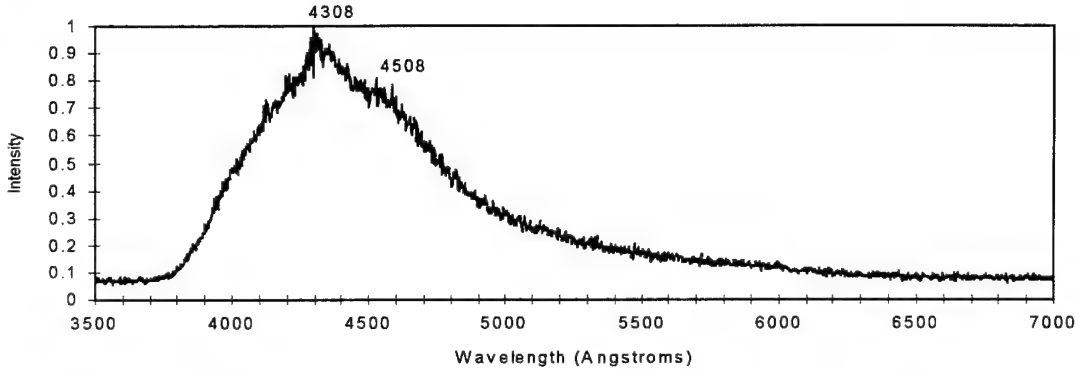

Figure 12b: Spectrum of an 8E-7 A, 0.5 MeV H3+ excited gel (P=2E-5 torr) observed 1 mm downstream from the upstream surface of the gel (Area B).

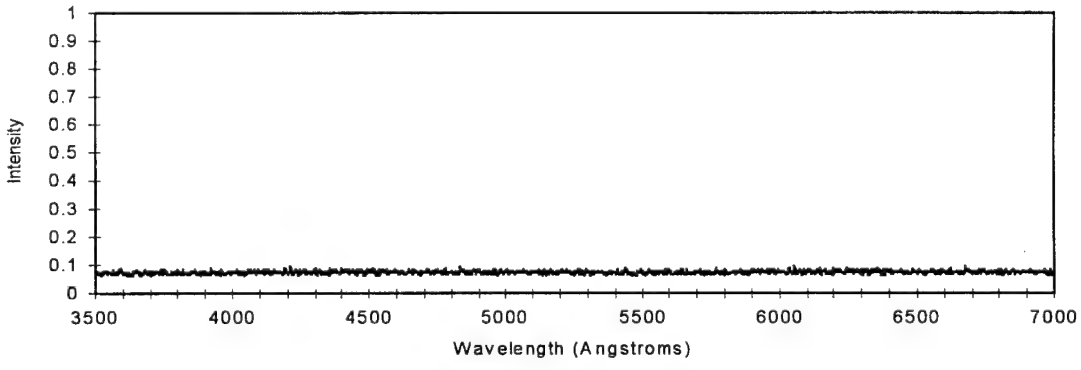

Figure 12c: Spectrum of an 8E-7 A, 0.5 MeV H3+ excited gel (P=2E-5 torr) observed 2 mm downstream from the downstream surface of the gel (Area C).

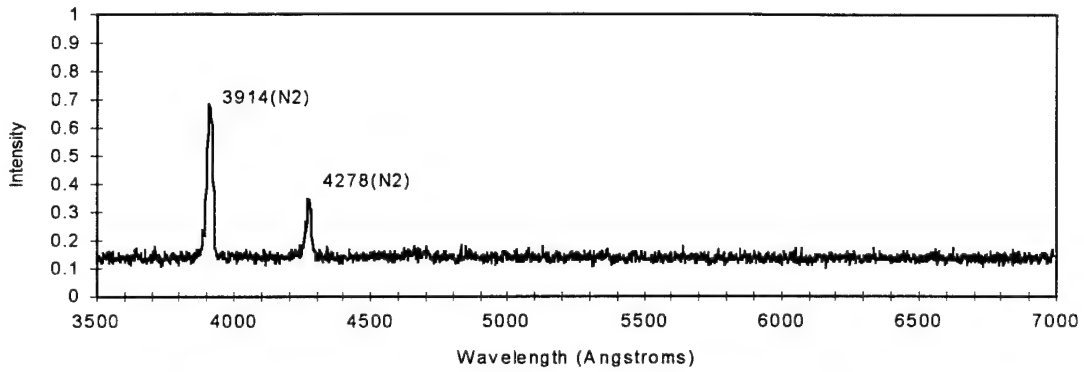

Figure 13a: Spectrum of a 4.5E-7 A, 0.5 MeV H3+ excited gel (P=1.2E-4 torr) observed 1 mm upstream from the upstream surface of the gel (Area A).

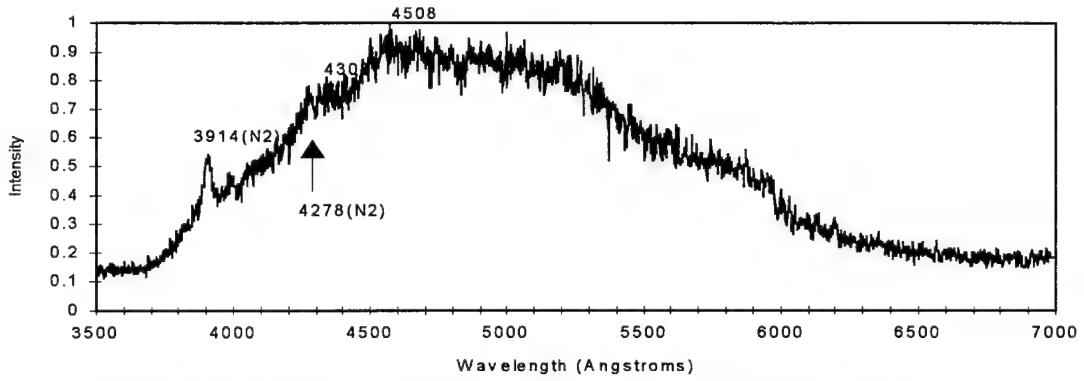

Figure 13b: Spectrum of a 4.5E-7 A, 0.5 MeV H3+ excited gel (P=1.2E-4 torr) observed 1 mm downstream from the upstream surface of the gel (Area B).

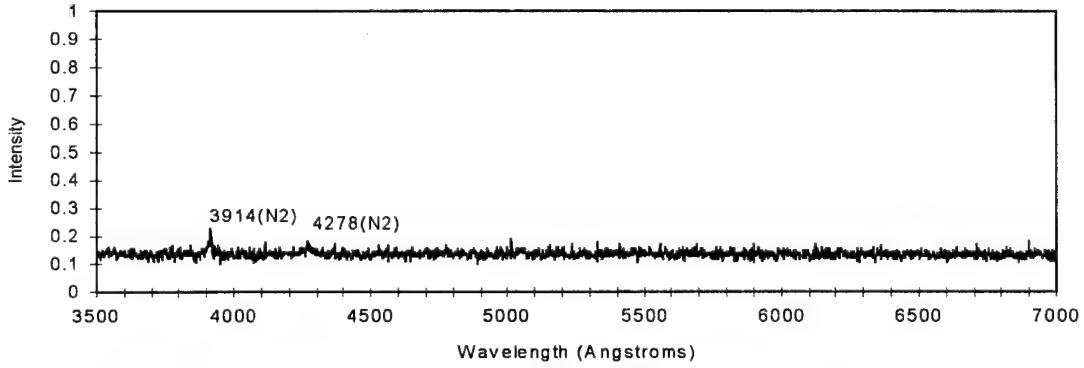

Figure 13c: Spectrum of 4.5E-7 A, 0.5 MeV H3+ excited gel (P=1.2E-4 torr) observed 2 mm downstream from the downstream surface of the gel(Area C).

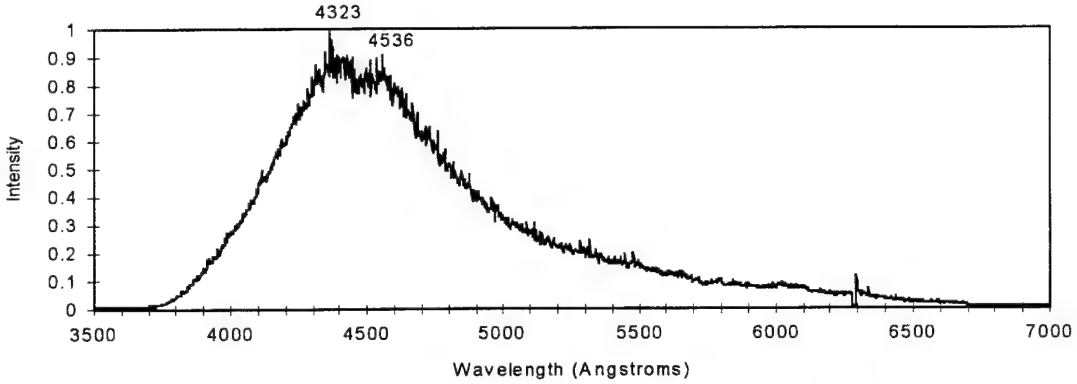

Figure 14a: Spectrum of a 4E-7 A, 0.5 MeV H+ excited gel (P=2E-5 torr) observed 1 mm downstream from the upstream surface of the gel (Area B).

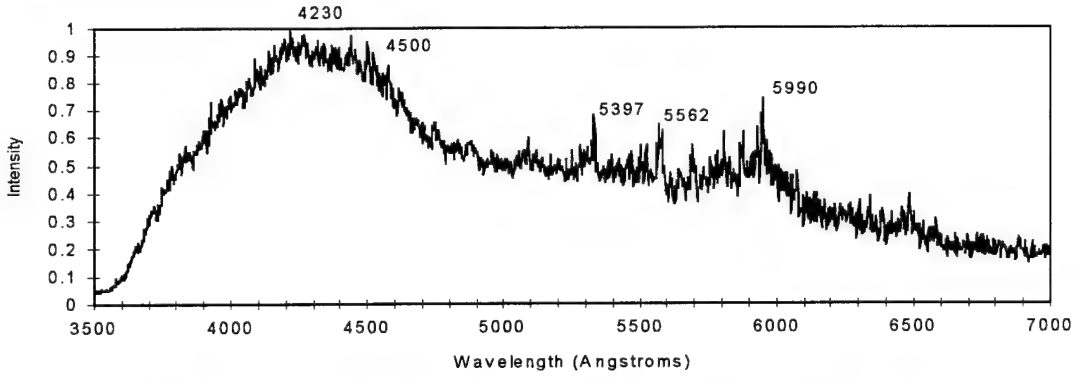

Figure 14b: Spectrum of a 9E-7 A, 0.5 MeV H2+ excited gel (P=2E-5 torr) observed 1 mm downstream from the upstream surface of the gel (Area B).

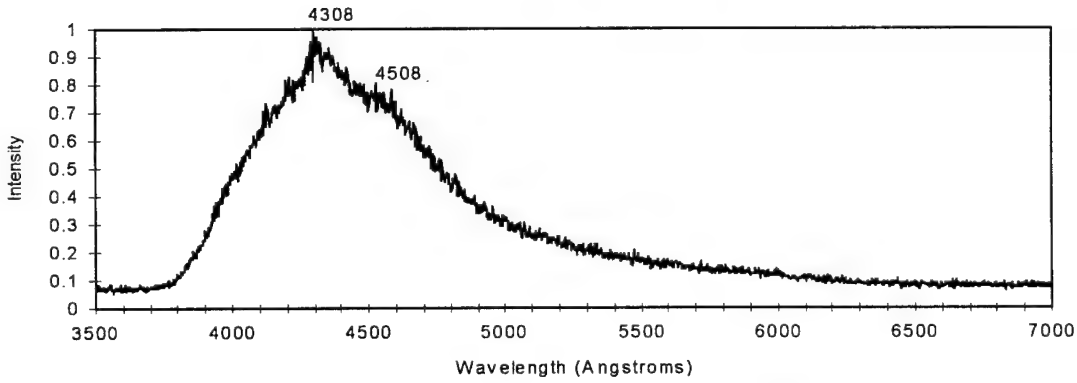

Figure 14c: Spectrum of an 8E-7 A, 0.5 MeV H3+ excited gel (P=2E-5 torr) observed 1 mm downstream from the upstream surface of the gel (Area B).

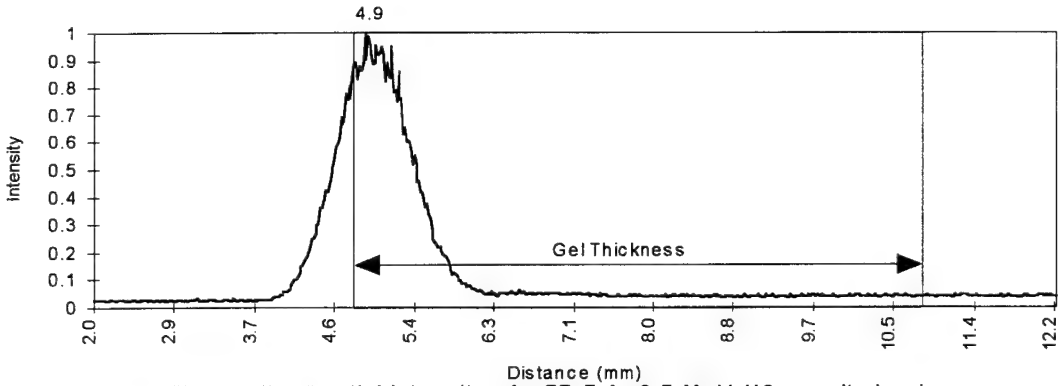

Figure 15a: Spatial intensity of a 7E-7 A, 0.5 MeV H3+ excited gel scanned at a set wavelength of 4500 angstroms.

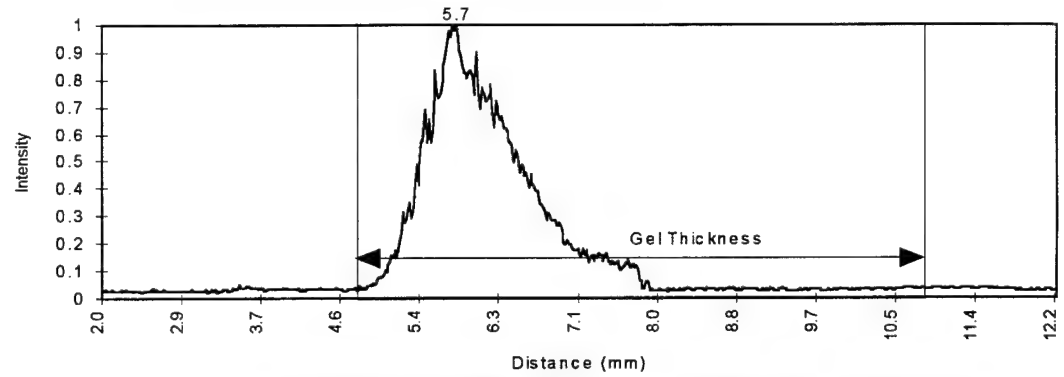

Figure 15b: Spatial intensity of a 6E-7 A, 0.75 MeV H3+ excited gel scanned at a set wavelength of 4500 angstroms.

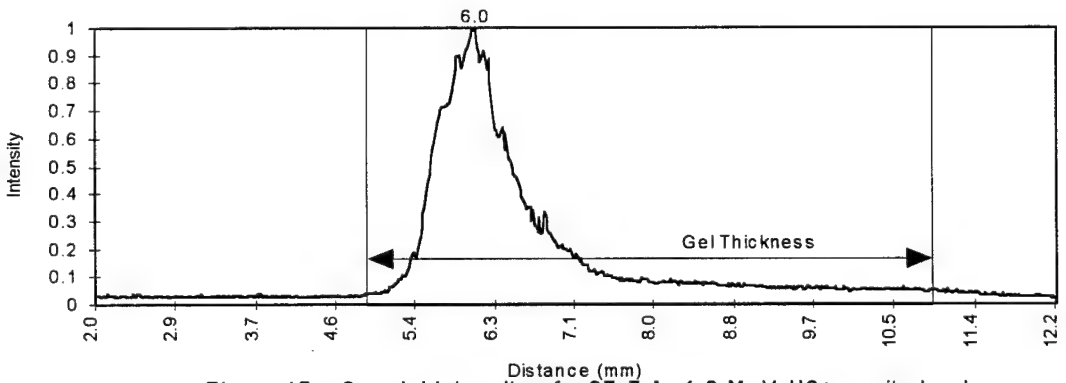

Figure 15c: Spacial intensity of a 6E-7 A, 1.0 MeV H3+ excited gel scanned at a set wavelength of 4500 angstroms.

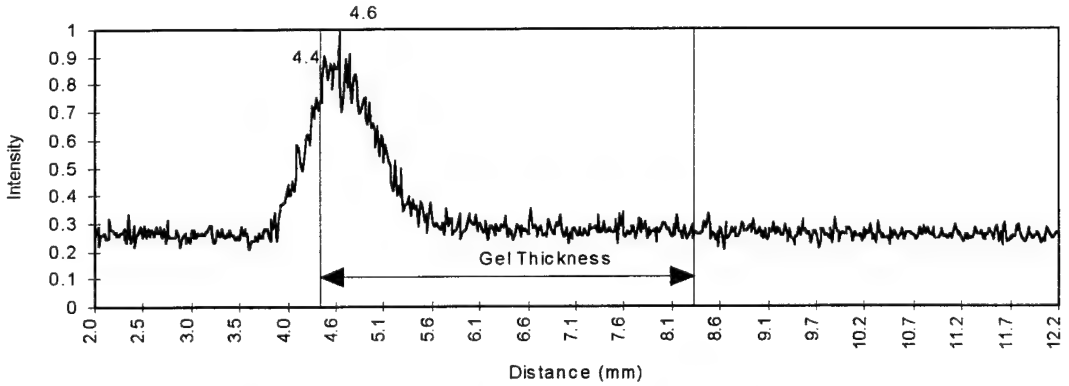

Figure 16a: Spacial intensity of a 5E-7 A, 0.5 MeV H3+ excited gel (P=1.2E-4 torr) scanned at a set wavelength of 4500 angstroms.

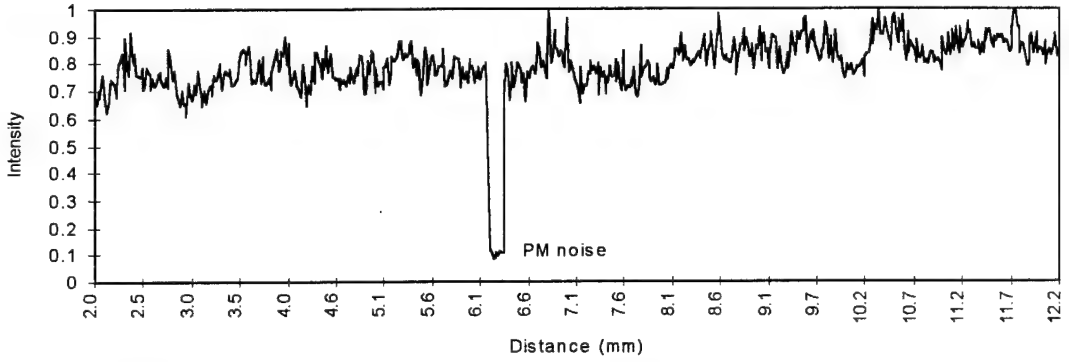

Figure 16b: Spacial intensity of 5E-7 A, 0.5 MeV H3+ excited air (w/o gel) (P=1.2E-4 torr) scanned at a set wavelength of 3900 angstroms.

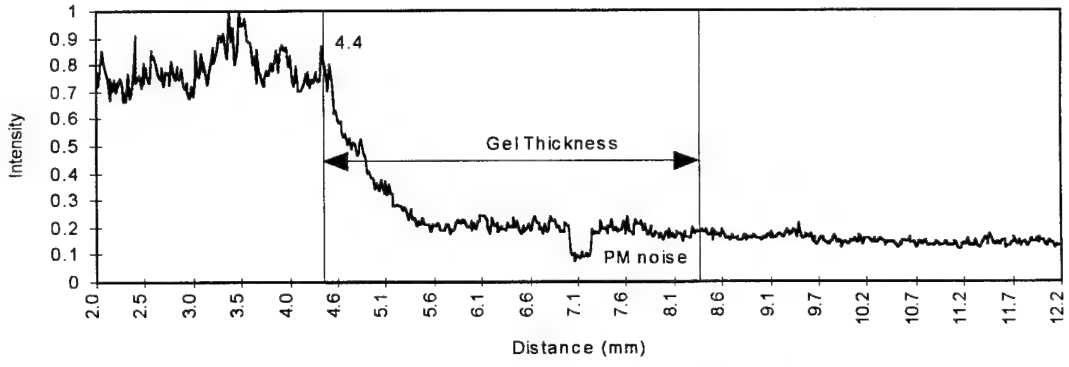

Figure 16c: Spacial intensity of a 5E-7 A, 0.5 MeV H3+ excited air (with gel) (P=1.2E-4 torr) scanned at a set wavelength of 3900 angstroms.

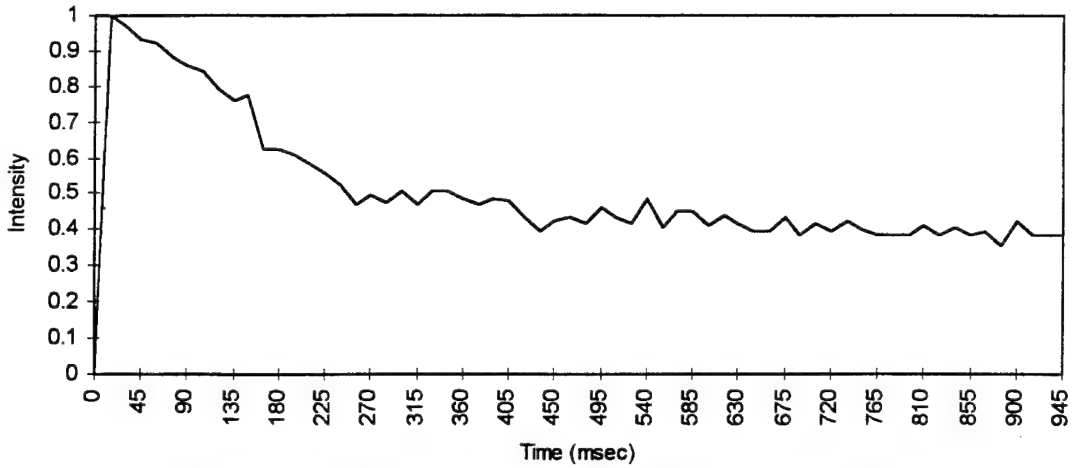

Figure 17a: Light pulse from a 6.2E-7 A, 0.5 MeV H3+ excited gel (P=2E-5 torr) with the beam initiated at 15 msec.

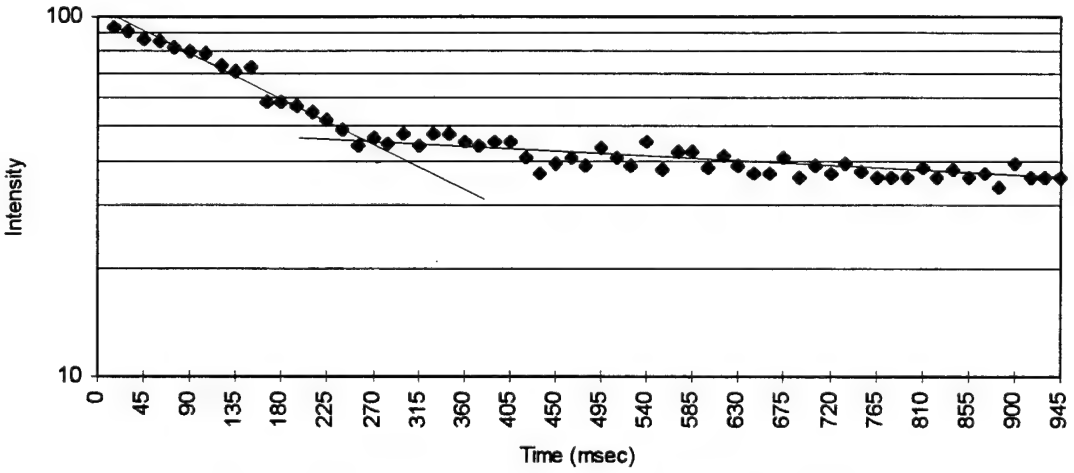

Figure 17b: Log plot of light pulse.
Decay constants: fast = -1.289/sec and slow = -0.250/sec.

8. DISCUSSION

8.1. Gel Spectral Characteristics

The physical characteristics of the aerogel were stated in Section 2. Now we discuss the spectral characteristics of the gel when subjected to a particle beam. First we will discuss some problems with the gel excitation experiments, and then point out some features of the gel while it is being subjected to a particle beam.

Once a gel was mounted, its useful life varied immensely, depending on the parameters of the experiment. Over time, the particle beam coated the gel, most likely with vapors from the pump oil, rendering it virtually useless. Some of the gels came out of the chamber completely discolored, or with holes in them (voiding the experiment). As the current of the particle beam increased, the deterioration of the gel increased. We used 0.5 μA currents in our experiments because it was low enough not to drastically damage the gel, yet high enough to give good data. The target chamber pressure also affected the useful life of the gel. Higher pressures (around 2×10^{-4} torr), greatly decreased the functional life time of the gel. The lowest possible pressures were used that could give the desired results while gel bombardment time was kept to a minimum. The deterioration of the gel was also increased with increasing beam particle energy. Most of our

experiments were done at 0.5 MeV. That energy was low enough to decrease the gel deterioration, but high enough to give good results.

The gel had an interesting spectrum. Comparing it to those from published beam-gas and beam-foil experiments, there seems to be little new information. Beam excitation of the residual air gives a continuous spatial intensity throughout the entire chamber (Figure 16b). Beam-foil shows a constant spatial intensity decay downstream. The gel had a continuous excitation of the air inside the gel that deteriorated as the beam traversed the gel (Figure 16c).

The gel spectra depended on the particle incident on the gel. The H^+ (Figure 14a) and H_3^+ (Figure 14c) spectra were similar, while the H_2^+ (Figure 14b) spectrum was quite unique. The H_3^+ particle was used for most of the experiments because it was relatively abundant in the Van de Graaff. The gel spectra did not depend on beam current. Beam penetration into the gel increased as the particle energy increased, as can be seen in figure 15. A very small fraction of the current was found to penetrate the gel even though looking at the mass-per-unit-area comparisons in Section 3 would make it seem highly unlikely. The current penetration may be due to the fact that the gel does not have a crystal structure, so it could be possible for particles to pass through the gel via the prevalent pores.

The spatial intensity of the gel slowly increased with increasing distance into the gel, reached a peak, and then decreased (Figure 16a). The peak location depended on the energy and the beam particle (H_3^+ is shown in figure 15). Figure 16b and figure 13 show that the beam-air experiment's spatial intensity remains relatively constant. By examining the beam-air's spatial intensity inside the gel, figure 16c, it is possible to see how the intensity seems to decrease as it traverses the gel. That would seem to imply a decrease in gas excitation which could be a result of beam scattering.

8.2. Gel Radiation Source

Section 4 listed several radiation sources along with their governing equations and characteristic properties. Now we can compare the characteristics of those radiations with those observed from the aerogel to see if similar processes occur.

The Bethe-Bloch equation may be the most applicable to explain the aerogel spectra. The spatial intensity of the air spectral lines decays as they pass through the gel (Figure 16c). The spatial intensity migrates deeper into the gel as particle energy, and thus the velocity, increases (Figure 15). The absorbed energy emitted from the gel is a continuum, a characteristic of a transparent solid subjected

to electromagnetic radiation experiencing excitation according to the Bethe-Bloch equation.

The spectral continuum from the gel peaked in the blue, λ4508 Å (Figure 8d). The continuum cannot be attributed to broadening of discrete spectral lines, because at the higher chamber pressures the spectral lines from the air in the gel were not broadened (Figure 13b).

The continuum peak wavelength in the blue is far from the peak wavelength of the black body radiations seen at low temperature's at λ5890 Å (Figure 8b), and at high temperature's at λ5478 Å (Figure 8c). Figure 8b and 8c, show a small variation with voltage, but both peaks remain in the red spectral region. Since the gel's continuum has its peak wavelength in the blue spectral region it is unlikely that the continuum is due to black body radiation.

Figure 9 shows an increase in intensity between the Plexiglas platform without the gel (Figure 9a) and with the gel (Figure 9b) illuminated with a mercury lamp. This could suggest a form of luminescence occurring, but the spectral line intensities have also changed. The difference could be attributed to an increase in light. Quartz luminesces in the blue spectral region. Figure 10 shows that a beam-quartz spectrum (Figure 10a) is almost identical to that of the gel (Figure 10b). This indicates that the gel spectrum

is also from a form of luminescence; whether it is fluorescence or phosphorescence is difficult to tell. The Quartz is made of silicon and fluoresces in the blue spectral region. The gel is likewise made of silicon and has shown to luminesce in the blue spectral region, so the gel seems to be showing the fluorescence characteristic of silicon.

Figure 17a shows the light pulses experienced by the gel when initially subjected to the particle beam. The burst of light is followed by a very fast and then a slower decay of radiation at λ4500 Å. Figure 17b, a log plot of the intensities, gives a value of 0.8 sec for the fast decay and 4 sec for the slow decay. This is a characteristic displayed by most scintillators.

Cherenkov radiation deals with particles moving at very high velocities. With the index of refraction for the aerogel, the particles would have to travel around 2.3×10^8 to 3×10^8 m/sec (almost the speed of light itself). Our velocities ranged from only 4.00×10^6 to 1.70×10^7 m/sec and are not sufficient for the criteria for Cherenkov radiation. Aerogels have been used as scintillators in the Cherenkov detectors where decay times are associated with scintillator properties. A cosmic ray penetrating the gel at a speed near the speed of light causes a pulse of light from the excitation due to the Cherenkov effect.

Bremsstrahlung radiation comes from accelerated electrons. Because of the heavier particles used in our experiments (over 1836 times more massive than the electron) and lower speeds, Bremsstrahlung radiation is minimal. Synchrotron radiation is essentially Bremsstrahlung radiation and does not pertain to the experiments performed.

9. CONCLUSION

The aerogel is a very peculiar chunk of solid "nothing." We discussed several new applications of the material and some possible experiments for further study. This work shows that the possibility of enhancing the science of particle beam physics is highly unlikely. Although particle beam physics with gels might unlock some of the gel's secrets, its application to particle beam research does not seem particularly useful.

Particle beams might be used to find trends in different gel structures useful for particular applications. The experiments performed in this thesis were done on a silicon aerogel. Different aerogels may give more revealing and interesting results. The gel might give information about the penetration of ions through matter and the random manner in which particles traverse a solid.

NOTES

[1]Kevin J. Anderson, "Historical Note: From Aqua Gel to Aerogel," MRS Bulletin (March 1991): 63.

[2]Anderson 63.

[3]Anderson 64.

[4]"Aerogels: Solid Pieces of Nothing," Compressed Air Magazine (June 1989): 28.

[5]Arlon Hunt, "Aerogels: The Lightest Solid," Encyclopedia Britannica 1995 Science Year Book, 1.

[6]"Aerogels" 31.

[7]Jeffery Kahn, "Innovative Insulators," LBL Research Review, (Summer 1991): 8.

[8]"Aerogels" 28.

[9]Anderson 63.

[10]"Aerogels" 28.

[11]Anderson 63-64.

[12]W. S. C. Williams, Nuclear And Particle Physics (Oxford: Clarendon, 1991) 36.

[13]Stanley Humphries, Jr., Principles of Charged Particle Acceleration (New York: Wiley & Sons, 1986).

[14]Stanley Bashkin, ed., Beam-Foil Spectroscopy: Proceedings of the Third International Conference on Beam-Foil Spectroscopy (Amsterdam: North-Holland, 1973).

[15]Stanley Bashkin, ed., Beam-Foil Spectroscopy, 2 Vols. (New York: Gordan, 1968) 2.

[16]Williams 6-8.

[17]Williams 47.

[18]Williams 47.

[19]Williams 235- 246.

[20]Williams 245.

[21]Raymond A. Serway, Clement J. Moses, and Curt A. Moyer, Modern Physics (Philadelphia: Saunders College, 1989) 43.

[22]Serway 45.

[23]Serway 47.

[24]Serway 44.

[25]S. C. Curran, Luminescence and the Scintillation Counter (New York: Academic, 1953) 72-74.

[26]Curran 83-85.

[27]Ralph S. Becker, Theory and Interpretation of Fluorescence and Phosphorescence (New York: Wiley Interscience, 1969) 1-3.

[28]Williams 247-249.

[29]G. F. G. Delaney, and E. C. Finch. Radiation Detectors: Physical Principles and Applications (Oxford: Clarendon, 1992) 327-329.

[30]Humphries 535.

[31]Sune Svanberg, Atomic and Molecular Spectroscopy: Basic Aspects and Practical Applications, Vol. 6 of Springer Series on Atoms+Plasmas, 8 Vols. (Heidelberg: Springer-Verlae, 1991) 96.

[32]Instruction Manual HVI-475M1: The Model AN-2000 Positive Ion Accelerator (HV Engineering: Burlington, n.d).

[33]Scanning Monochrometer EU-700 and EUE-700 Series (Benton Harbor: Heath, 1969).

WORKS CITED

"Aerogels: Solid Pieces of Nothing." Compressed Air Magazine. June 1989: 27-31.

Anderson, Kevin J. "Historical Note: From Aqua Gel to Aerogel." MRS Bulletin. March 1991: 63-64.

Bashkin, Stanley, ed. Beam-Foil Spectroscopy. 2 Vols. New York: Gordan, 1968. Vol. 2.

Bashkin, Stanley, ed. Beam-Foil Spectroscopy: Proceedings of the Third International Conference on Beam-Foil Spectroscopy. Amsterdam: North-Holland, 1973.

Becker, Ralph S. Theory and Interpretation of Fluorescence and Phosphorescence. New York: Wiley Interscience, 1969.

Birks, J. B. The Theory and Practice of Scintillation Counting. New York: Macmillan, 1964.

Curran, S. C. Luminescence and the Scintillation Counter. New York: Academic, 1953.

Delaney, G. F. G., and E. C. Finch. Radiation Detectors: Physical Principles and Applications. Oxford: Clarendon, 1992.

Humphries, Stanley, Jr. Principles of Charged Particle Acceleration. New York: Wiley & Sons, 1986.

Hunt, Arlon. "Aerogels: The Lightest Solid." Encyclopedia Britannica 1995 Science Year Book.

Instruction Manual HVI-475M1: The Model AN-2000 Positive Ion Accelerator. HV Engineering: Burlington, n.d.

Kahn, Jeffery. "Innovative Insulators." LBL Research Review. Summer 1991: 2-9.

Scanning Monochrometer EU-700 and EUE-700 Series. Benton Harbor: Heath, 1969.

Serway, Raymond A., Clement J. Moses, and Curt A. Moyer. Modern Physics. Philadelphia: Saunders College, 1989.

Svanberg, Sune. Atomic and Molecular Spectroscopy: Basic Aspects and Practical Applications. Vol. 6 of Springer Series on Atoms+Plasmas. 8 Vols. Heidelberg: Springer-Verlae, 1991.

Tatarskii, V. I., et al, ed. Wave Propagation in Random Media (Scintillation). Bellingham: SPIE, 1993.

Weber, Marvin J., et al, ed. Scintillator and Phosphor Materials. Vol. 348 of Materials Research Society Symposium Proceedings. Pittsburg: MRS, 1994.

Williams, W. S. C. Nuclear And Particle Physics. Oxford: Clarendon, 1991.